

AD-764 085

INELASTIC BUCKLING OF A DEEP SPHERICAL
SHELL SUBJECT TO EXTERNAL PRESSURE

N. C. Huang, et al

Notre Dame University

Prepared for:

Office of Naval Research

July 1973

DISTRIBUTED BY:

NTIS

National Technical Information Service
U. S. DEPARTMENT OF COMMERCE
5285 Port Royal Road, Springfield Va. 22151

AD 764085



DISTRIBUTION OF THIS DOCUMENT IS UNLIMITED

Deep Ocean Engineering

CONTRACT ONR-N00014-68-A-0152

University of Notre Dame

college of engineering

notre dame, indiana

46556

~~NOT PHOTOGRAPH THIS PAGE~~

~~RECEIVED~~
AUG 2 1973

~~B~~

AD-768085

INELASTIC BUCKLING OF A DEEP SPHERICAL
SHELL SUBJECT TO EXTERNAL PRESSURE

by

N. C. Huang and G. Funk

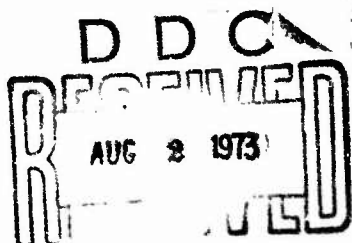
July, 1973

Document cleared for public release and sale:

Distribution is unlimited.

University of Notre Dame
College of Engineering
Notre Dame, Indiana 46556

Contract
N00014-68-A-0152(NR 260-112/7-13-67)
Office of Naval Research



TECHNICAL REPORT
NUMBER: UND-73-7

FOREWORD

This technical report was prepared by the Dynamical Systems Group under the Deep Sea Engineering Project at the University of Notre Dame, College of Engineering. The authors, N. C. Huang and G. Funk are Professor and Graduate Research Assistant in the Department of Aerospace and Mechanical Engineering.

The research was performed under the sponsorship of the Department of the Navy, Office of Naval Research, Washington, D.C. 20360, with funding under Contract N00014-68-A-0152 and In-House Account Number UND-2400-24038.

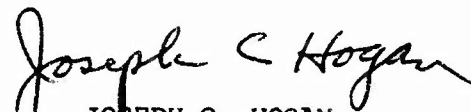
The authors wish to express their appreciation to Mrs. Josephine Peiffer for her careful typing of the manuscript.

Readers are advised that reproduction in whole or in part is permitted for any purpose of the United States Government.

This technical report has been reviewed and approved for submittal to the sponsoring agency July, 1973.



EDWARD W. JERGER
PROGRAM MANAGER



JOSEPH C. HOGAN
DEAN, COLLEGE OF ENGINEERING
UNIVERSITY OF NOTRE DAME

UNCLASSIFIED

Security Classification

DOCUMENT CONTROL DATA - R&D

(Security classification of title, body of abstract and indexing annotation must be entered when the overall report is classified.)

1. ORIGINATING ACTIVITY (Corporate author) College of Engineering University of Notre Dame Notre Dame, Indiana 46556		2a. REPORT SECURITY CLASSIFICATION UNCLASSIFIED	
		2b. GROUP	
3. REPORT TITLE Inelastic Buckling of a Deep Spherical Shell Subject to External Pressure			
4. DESCRIPTIVE NOTES (Type of report and inclusive dates)			
5. AUTHOR(S) (Last name, first name, initial) N. C. Huang and G. Funk			
6. REPORT DATE July, 1973		7a. TOTAL NO. OF PAGES 5869	7b. NO. OF REFS 11
8a. CONTRACT OR GRANT NO. N00014-68-A-0152		9a. ORIGINATOR'S REPORT NUMBER(S) UND-73-7	
b. PROJECT NO. In-House Account No. 2400-24038		9b. OTHER REPORT NO(S) (Any other numbers that may be assigned this report)	
d.			
10. AVAILABILITY/LIMITATION NOTICES Document cleared for public release and sale. Its distribution is unlimited.			
11. SUPPLEMENTARY NOTES		12. SPONSORING MILITARY ACTIVITY Department of the Navy	
13. ABSTRACT This paper is concerned with the investigation of the inelastic buckling of a deep spherical shell subject to a uniformly distributed external pressure. The geometry of the shell is considered to be axisymmetrical while the shell thickness may vary as a function of the polar angle. The edge of the shell is supported elastically. The material of the shell is assumed to satisfy the generalized Ramberg-Osgood stress-strain relations and a power law of steady creep. The analysis is based on Sanders' non-linear theory of thin shells expressed in an incremental form and Hill's theory of inelastic bifurcation. Computations are carried out by a numerical iterative procedure associated with a finite difference method. Solutions are sought for both the axisymmetrical inelastic buckling and the asymmetrical bifurcation.			

KEY WORDS

LINK A		LINK B		LINK C	
ROLE	WT	ROLE	WT	ROLE	WT

INELASTIC BIFURCATION
 SUBMERGED DEEP SPHERICAL SHELL
 RAMBERG-OSGOOD MATERIAL
 STEADY CREEP

ib

ABSTRACT

This paper is concerned with the investigation of the inelastic buckling of a deep spherical shell subject to a uniformly distributed external pressure. The geometry of the shell is considered to be axisymmetrical while the shell thickness may vary as a function of the polar angle. The edge of the shell is supported elastically. The material of the shell is assumed to satisfy the generalized Ramberg-Osgood stress-strain relations and a power law of steady creep. The analysis is based on Sanders' nonlinear theory of thin shells expressed in an incremental form and Hill's theory of inelastic bifurcation. Computations are carried out by a numerical iterative procedure associated with a finite difference method. Solutions are sought for both the axisymmetrical inelastic buckling and the asymmetrical bifurcation.

NOMENCLATURE

a_{ij}	elastic support constants
\underline{A} , \underline{B} , \underline{D} , \underline{E} , \underline{F}	matrices defined in Appendix A
C_{ij} , c_{ij}	coefficients in constitutive relations
\underline{c}	matrix of c_{ij}
D_i , d_i	steady creep strain rate
\underline{d}	vector of d_i
E	Young's modulus
E_{ij} , e_{ij}	membrane strains
\bar{E}_{ij} , \bar{e}_{ij}	strain components in the shell
$F(\sigma_e)$, $F(\tau_e)$	creep functions
\underline{f}	\underline{c}^{-1}
f_{ij}	elements of \underline{f}
G , g	constants in constitutive equations
\underline{g}	$\underline{f} \underline{d}$
g_i	elements of \underline{g}
h , η	shell thickness
h_0	reference thickness
\underline{I} , \underline{J}	matrices whose elements are integrals of moments of f_{ij} and g_i
I_{ij} , J_i	elements of \underline{I} and \underline{J}
J_2 , j_2	second invariant of the stress tensor
K_{ij} , k_{ij}	bending strains
\underline{K} , \underline{L} , \underline{M} , \underline{R} , \underline{U} , \underline{V}	matrices defined in section 3

m	constant in the steady creep relation
M_{ij}, m_{ij}	moment resultants
N_i, n_i	membrane forces
n	bifurcation mode
n_m	number of meridional increments
n_r	constant in the Ramberg-Osgood relation
P, p	external pressure
\tilde{P}_i	matrix defined in section 3
Q_i, q_i	transverse shear resultant
\tilde{Q}_i	matrix defined in section 3
R	radius of the middle surface
\tilde{S}	$[n_{11} \ n_{22} \ m_{11} \ m_{22}]^T$
U_i, u_i	tangential displacements
W, w	outward normal displacement
W_L, W_N	linear and nonlinear potential functions
z, ζ	radial distance from the shell middle surface
$\tilde{\alpha}_i, \tilde{\beta}_i$	matrices defined in section 3
β	longitude (see Fig. 1)
γ	a constant
Δ	meridional increment
δ	a constant
$\tilde{\epsilon}$	$[\epsilon_{11} \ \epsilon_{22} \ \kappa_{11} \ \kappa_{22}]^T$
θ	polar angle (see Fig. 1)
λ	h/R
ν	Poisson's ratio

σ_{ij}, τ_{ij}	stress components at any position in the shell
σ_e, τ_e	effective stresses
σ_c, τ_c	material constants in the creep relation
σ_o, τ_o	materials constants in the Ramberg-Osgood equation
φ	rotation about the outward normal
φ_i	rotations about the surface tangents
(\sim)	symmetrical quantities associated with the fundamental solution
$(\overline{\quad}), (\quad)^*$	asymmetric quantities
$(\quad)_i$	finite difference quantities

TABLE OF CONTENTS

	page
1. INTRODUCTION - - - - -	1
2. BASIC EQUATIONS - - - - -	3
3. AXISYMMETRICAL DEFORMATION - - - - -	12
4. ASYMMETRICAL BIFURCATION - - - - -	18
5. RESULTS AND DISCUSSIONS - - - - -	25
6. CONCLUDING REMARKS - - - - -	29
7. REFERENCES - - - - -	30
APPENDIX A - - - - -	32
APPENDIX B - - - - -	34
APPENDIX C - - - - -	38

LIST OF FIGURES

	page
Fig. 1 The geometry of the shell.	49
Fig. 2 \bar{w}_{ave} vs. t curves.	50
Fig. 3 \bar{u}_1 vs. θ curves for $p = 0.005194$ and 0.007420 .	51
Fig. 4 \bar{w} vs. θ curves for $p = 0.005194$ and 0.007420 .	52
Fig. 5 \bar{n}_{11} vs. θ curves for $p = 0.005194$ and 0.007420 .	53
Fig. 6 \bar{n}_{22} vs. θ curves for $p = 0.005194$ and 0.007420 .	54
Fig. 7 \bar{q}_1 vs. θ curves for $p = 0.005194$ and 0.007420 .	55
Fig. 8 \bar{m}_{11} vs. θ curves for $p = 0.005194$ and 0.007420 .	56
Fig. 9 \bar{m}_{22} vs. θ curves for $p = 0.005194$ and 0.007420 .	57
Fig.10 p vs. \bar{w}_{ave} curve.	58

1. INTRODUCTION

In recent years, new developments in deep ocean exploration demand further refinement and sophistication in the design of submersibles. An important problem encountered in the design of submerged hulls is the selection of a suitable material with high-strength and low-density properties. In view of the nature of the material available and due to the limitations on structural weight, it is necessary that an accurate stress analysis of the hull and a reliable prediction of the collapse load be established.

When the submerged depth is large, the configuration of the hull is usually spherical. The spherical shell can provide a good structural layout from the viewpoint of stress analysis. Furthermore, it has the advantage of low drag during the motion of the hull. CNR's vehicle ALVIN is a typical example of the spherical hull. For this type of pressure hull, when it is submerged to a large depth, the deformation of the hull may become finite and the state of stress in the hull may reach the inelastic range. In a critical condition, structural failure may occur as a result of inelastic buckling.

Since Shanley first introduced the concept of inelastic bifurcation of a column under increasing axial compressive load [1], substantial progress has been made in the field of inelastic buckling of structures. Research along this line can be found in a comprehensive survey paper prepared by Sewell [2]. The general study of the inelastic stability of solids based on the concept of

uniqueness of solution was given by Hill [3,4]. He concludes that Shanley's concept of inelastic buckling under increasing load is a natural sequel to his general theory. In Hill's work, a variational principle is established for finite deformation of inelastic solids based on the existence of convex plastic potential surface. This variational principle is essentially an extension of the well-known principle of minimum potential energy in finite elasticity. Hill's variational principle incorporated with Rayleigh-Ritz technique or Galerkin technique has been employed for the analysis of inelastic buckling of thin shells [5,6,7].

Similar to the case of elastic buckling, the critical condition for inelastic buckling is usually sensitive to the initial imperfections existing in the structural geometry or loading condition. In fact, for many structures, such as columns and complete spherical shells, the inelastic bifurcation occurs only when the geometry of the structure and the loading condition are perfect. With imperfections, bifurcation disappears although the collapse load can still exist. It is found that the magnitude of the collapse load depends strongly on the imperfection of the structure [8,9]. This behavior of imperfection-sensitivity indicates that the analytical results derived from the variational principle may depend on the assumed deflection function used in the Rayleigh-Ritz technique. To remedy the deficiency introduced by the Rayleigh-Ritz technique, the problem of inelastic stability of shells can be investigated directly from the governing nonlinear

shell equations. Typical examples of this approach are found in [9,10].

In this paper, we shall deal with the problems of axisymmetrical collapse and asymmetrical bifurcation of a deep spherical shell in the inelastic range introduced by a uniform external pressure. The model of spherical shell use in our analysis is chosen to be close to the actual shell configuration of the ALVIN vehicle. The thickness distribution of the shell is regarded as axisymmetrical but variable as a function of the polar angle θ . The edge of the shell is considered to be elastically supported. The shell material is assumed to be isotropic satisfying Ramberg-Osgood stress-strain relations and a power law of steady creep. Our analysis is based on the Kirchhoff assumption with small strains. Sanders' nonlinear theory for finite deformation of thin shells [11] will be employed in our formulation.

2. BASIC EQUATIONS

Consider a deep spherical shell with radius of the middle surface R subjected to a uniform external pressure P . Let us introduce surface polar spherical coordinates with polar angle θ and longitude β as shown in Figure 1. In the following, we shall take θ and β as the parametric coordinates. Thus our lines of curvature are meridional lines and circles perpendicular to the polar axis. The edge of the shell is specified by the circle $\theta = \theta_0$. We shall assume that the thickness distribution of the shell is axisymmetrical, i.e. $h = h(\theta)$.

Let us denote the components of displacement in the meridional, circumferential and outward normal directions by U_1 , U_2 , and W respectively. According to Sanders' nonlinear theory of shells [11], the components of rotation in the directions of tangents and normal to the middle surface are given respectively by

$$\varphi_1 = \frac{1}{R}(U_1 - W_{,1}), \quad (1)$$

$$\varphi_2 = \frac{1}{R}(U_2 - W_{,2} \csc \theta), \quad (2)$$

$$\varphi = \frac{1}{2R}(U_2 \cot \theta + U_{2,1} - U_{1,2} \csc \theta), \quad (3)$$

where $()_{,1} \equiv \frac{\partial}{\partial \theta} ()$ and $()_{,2} \equiv \frac{\partial}{\partial \beta} ()$. The membrane strains are

$$E_{11} = \frac{1}{R}(W + U_{1,1}) + \frac{1}{2}(\varphi_1^2 + \varphi^2), \quad (4)$$

$$E_{22} = \frac{1}{R}(W + U_1 \cot \theta + U_{2,2} \csc \theta) + \frac{1}{2}(\varphi_2^2 + \varphi^2), \quad (5)$$

$$E_{12} = \frac{1}{2R}(U_{2,1} + U_{1,2} \csc \theta - U_2 \cot \theta + R \varphi_1 \varphi_2). \quad (6)$$

The bending strains are

$$K_{11} = \frac{1}{R} \varphi_{1,1}, \quad (7)$$

$$K_{22} = \frac{1}{R}(\varphi_{2,2} \csc \theta + \varphi_1 \cot \theta), \quad (8)$$

$$K_{12} = \frac{1}{2R}(\varphi_{2,1} + \varphi_{1,2} \csc \theta - \varphi_2 \cot \theta). \quad (9)$$

Let us denote the components of membrane force, transverse shear and moment resultant by N_{11} , N_{22} , N_{12} , Q_1 , Q_2 , M_{11} , M_{22} and M_{12} . The equations of equilibrium of the deformed shell are

$$N_{11,1} + N_{11} \cot \theta + N_{12,2} \csc \theta - N_{22} \cot \theta + Q_1 - (\varphi_1 N_{11} + \varphi_2 N_{12}) \\ - \frac{1}{2} [\varphi(N_{11} + N_{22})]_{,2} \csc \theta - RP \varphi_1 = 0, \quad (10)$$

$$N_{22,2} + 2N_{12} \cos \theta + N_{12,1} \sin \theta + Q_2 \sin \theta - (\varphi_2 N_{22} + \varphi_1 N_{12}) \sin \theta \\ + \frac{1}{2} [\varphi(N_{11} + N_{22})]_{,1} \sin \theta - RP \varphi_2 \sin \theta = 0, \quad (11)$$

$$Q_{1,1} + Q_1 \cot \theta + Q_{2,2} \csc \theta - (N_{11} + N_{22}) - (\varphi_1 N_{11} + \varphi_2 N_{12})_{,1} \\ - (\varphi_1 N_{11} + \varphi_2 N_{12}) \cot \theta - (\varphi_1 N_{12} + \varphi_2 N_{22})_{,2} \csc \theta - RP = 0, \quad (12)$$

$$M_{11,1} + M_{11} \cot \theta + M_{12,2} \csc \theta - M_{22} \cot \theta - RQ_1 = 0, \quad (13)$$

$$M_{22,2} + 2M_{12} \cos \theta + M_{12,1} \sin \theta - RQ_2 \sin \theta = 0. \quad (14)$$

These equations are self-consistent in a sense that the principle of virtual work can be satisfied. Note that nonlinearity is introduced through the strain-displacement relations and equations of equilibrium.

By the Kirchhoff assumption, the strain components \bar{E}_{ij} ($i = 1, 2$; $j = 1, 2$) at any point in the shell with a distance z measured from the middle surface can be expressed in terms of the membrane strains and bending strains as

$$\bar{E}_{ij} = E_{ij} + z K_{ij}, \quad (15)$$

In Eq. (15), we consider that the shell is sufficiently thin.

Hence only the linear term in z is retained. Denote the stress

components at any point in the shell by σ_{ij} ($i = 1, 2; j = 1, 2$).

In the following we shall assume that the strains are small although the deformation of the shell may be finite. The constitutive relations can be written as

$$\begin{bmatrix} \dot{E}_{11} \\ \dot{E}_{22} \\ \dot{E}_{12} \end{bmatrix} = \begin{bmatrix} C_{11} & C_{12} & C_{13} \\ C_{21} & C_{22} & C_{23} \\ C_{31} & C_{32} & C_{33} \end{bmatrix} \begin{bmatrix} \dot{\sigma}_{11} \\ \dot{\sigma}_{22} \\ \dot{\sigma}_{12} \end{bmatrix} + \begin{bmatrix} D_1 \\ D_2 \\ 0 \end{bmatrix}, \quad (16)$$

where

$$C_{11} = \frac{1}{E} + \frac{G}{9} (2\sigma_{11} - \sigma_{22})^2, \quad (17)$$

$$C_{22} = \frac{1}{E} + \frac{G}{9} (2\sigma_{22} - \sigma_{11})^2, \quad (18)$$

$$C_{33} = \frac{1+\nu}{E} + 2G\sigma_{12}^2, \quad (19)$$

$$C_{12} = C_{21} = -\frac{\nu}{E} + \frac{G}{9} (2\sigma_{11} - \sigma_{22})(2\sigma_{22} - \sigma_{11}), \quad (20)$$

$$C_{13} = C_{31} = \frac{G}{3} (2\sigma_{11} - \sigma_{22}) \sigma_{12}, \quad (21)$$

$$C_{23} = C_{32} = \frac{G}{3} (2\sigma_{22} - \sigma_{11}) \sigma_{12}, \quad (22)$$

$$D_1 = F(\sigma_e) (\sigma_{11} - \frac{1}{2} \sigma_{22}), \quad (23)$$

$$D_2 = F(\sigma_e) (\sigma_{22} - \frac{1}{2} \sigma_{11}), \quad (24)$$

E is the Young's modulus, ν is the Poisson's ratio and G is defined as

$$G = \begin{cases} \frac{9}{4J_2} \left(\frac{1}{E_t} - \frac{1}{E} \right) & \text{for } \dot{J}_2 \geq 0 \text{ and } J_2 = (J_2)_{\max}; \\ 0 & \text{for } \dot{J}_2 < 0 \text{ or } J_2 < (J_2)_{\max}, \end{cases} \quad (25)$$

E_t is the tangent modulus, J_2 is given as

$$J_2 = \sigma_{11}^2 + \sigma_{22}^2 - \sigma_{11} \sigma_{22} + 3\sigma_{12}^2, \quad (26)$$

$(J_2)_{\max}$ is the maximum value of J_2 in its history, σ_e is the effective stress defined by

$$\sigma_e = J_2^{1/2}. \quad (27)$$

The function $F(\sigma_e)$ is given by

$$F(\sigma_e) = \frac{1}{\sigma_c} \left(\frac{\sigma_e}{\sigma_c} \right)^{m-1}, \quad (28)$$

where m and σ_c are material constants. The constitutive equation, Eq. (16), is obtained by a generalization of the uniaxial stress-strain relation:

$$E_t \dot{\epsilon} = \begin{cases} E_t \dot{\sigma} + \left(\frac{\sigma}{\sigma_c} \right)^m & \text{for } \sigma \dot{\sigma} \geq 0; \\ E_t \dot{\sigma} + \left(\frac{\sigma}{\sigma_c} \right)^m & \text{for } \sigma \dot{\sigma} < 0, \end{cases} \quad (29)$$

with the assumption that the plastic and creep deformations are incompressible. In our study, we shall assume that the material of the shell satisfies Ramberg-Osgood stress-strain relation for elastic-plastic deformation. Hence the tangent modulus can be expressed as

$$E_t = E \left[1 + \frac{3}{7} n_r \left(\frac{\sigma_e}{\sigma_0} \right)^{n_r-1} \right]^{-1} \quad (30)$$

where σ_0 is the stress determined by the intercept of the uniaxial stress-strain curve with a straight line through the

origin with a slope $0.7E$ and n_r is a material constant.

When the shell is sufficiently thin, the membrane forces and moments are related to the stress components by

$$N_{ij} = \int_{-h/2}^{h/2} \sigma_{ij} dz \quad (31)$$

and

$$M_{ij} = \int_{-h/2}^{h/2} z \sigma_{ij} dz \quad (32)$$

Consider h_0 as a reference thickness. Let us introduce the following dimensionless quantities:

$$u_i = \frac{U_i}{h_0}, \quad w = \frac{W}{h_0}, \quad \epsilon_{ij} = \frac{R}{h_0} E_{ij}, \quad \kappa_{ij} = R K_{ij}, \quad (33)$$

$$\lambda = \frac{h_0}{R}, \quad \eta = \frac{h}{h_0}, \quad n_{ij} = \frac{N_{ij}}{E h_0}, \quad m_{ij} = \frac{M_{ij}}{E h_0^2}, \quad (34)$$

$$q_i = \frac{Q_i}{E h_0}, \quad p = \frac{PR}{E h_0}, \quad e_{ij} = \frac{R}{h_0} \bar{E}_{ij}, \quad \tau_{ij} = \frac{\sigma_{ij}}{E}, \quad (35)$$

$$\tau_c = \frac{\sigma_c}{E}, \quad \tau_o = \frac{\sigma_o}{E}, \quad e_t = \frac{E_t}{E}, \quad \zeta = \frac{z}{h_0}. \quad (36)$$

Our governing equations for the general deformation of the shell can be expressed in terms of these dimensionless quantities as

$$\varpi_1 = \lambda(u_1 - w_{,1}), \quad (37)$$

$$\varpi_2 = \lambda(u_2 - w_{,2} \csc \theta), \quad (38)$$

$$\varphi = \frac{\lambda}{2} (u_2 \cot \theta + u_{2,1} - u_{1,2} \csc \theta), \quad (39)$$

$$\varpi_{11} = w + u_{1,1} + \frac{1}{2\lambda} (\varpi_1^2 + \varphi^2), \quad (40)$$

$$e_{22} = w + u_1 \cot \theta + u_{2,2} \csc \theta + \frac{1}{2} \lambda (\varpi_2^2 + \varpi^2), \quad (41)$$

$$e_{12} = \frac{1}{2}(u_{2,1} + u_{1,2} \csc \theta - u_2 \cot \theta + \frac{1}{\lambda} \varpi_1 \varpi_2), \quad (42)$$

$$k_{11} = \varpi_{1,1}, \quad (43)$$

$$k_{22} = \varpi_{2,2} \csc \theta + \varpi_1 \cot \theta, \quad (44)$$

$$k_{12} = \frac{1}{2}(\varpi_{2,1} + \varpi_{1,2} \csc \theta - \varpi_2 \cot \theta), \quad (45)$$

$$n_{11,1} + n_{11} \cot \theta + n_{12,2} \csc \theta - n_{22} \cot \theta + q_1 - (\varpi_1 n_{11} + \varpi_2 n_{12}) - \frac{1}{2} [\varpi(n_{11} + n_{22})]_{,2} \csc \theta - p \varpi_1 = 0, \quad (46)$$

$$n_{22,2} + 2n_{12} \cos \theta + n_{12,1} \sin \theta + q_2 \sin \theta - (\varpi_2 n_{22} + \varpi_1 n_{12}) \sin \theta + \frac{1}{2} [\varpi(n_{11} + n_{22})]_{,1} \sin \theta - p \varpi_2 \sin \theta = 0, \quad (47)$$

$$q_{1,1} + q_1 \cot \theta + q_{2,2} \csc \theta - (n_{11} + n_{22}) - (\varpi_1 n_{11} + \varpi_2 n_{12})_{,1} - (\varpi_1 n_{11} + \varpi_2 n_{12}) \cot \theta - (\varpi_1 n_{12} + \varpi_2 n_{22})_{,2} \csc \theta - p = 0, \quad (48)$$

$$m_{11,1} + m_{11} \cot \theta + m_{12,2} \csc \theta - m_{22} \cot \theta - \frac{1}{\lambda} q_1 = 0, \quad (49)$$

$$m_{22,2} + 2m_{12} \cos \theta + m_{12,1} \sin \theta - \frac{1}{\lambda} a_2 \sin \theta = 0, \quad (50)$$

$$e_{ij} = \epsilon_{ij} + \zeta \kappa_{ij}, \quad (51)$$

$$\begin{bmatrix} \dot{e}_{11} \\ \dot{e}_{22} \\ \dot{e}_{12} \end{bmatrix} = \begin{bmatrix} c_{11} & c_{12} & c_{13} \\ c_{21} & c_{22} & c_{23} \\ c_{31} & c_{32} & c_{33} \end{bmatrix} \begin{bmatrix} \dot{\tau}_{11} \\ \dot{\tau}_{22} \\ \dot{\tau}_{12} \end{bmatrix} + \begin{bmatrix} d_1 \\ d_2 \\ 0 \end{bmatrix}, \quad (52)$$

$$c_{11} = \frac{1}{\lambda} \left[1 + \frac{g}{9} (2\tau_{11} - \tau_{22})^2 \right], \quad (53)$$

$$c_{22} = \frac{1}{\lambda} \left[1 + \frac{g}{9} (2\tau_{22} - \tau_{11})^2 \right], \quad (54)$$

$$c_{33} = \frac{1}{\lambda} (1 + \nu + 2g\tau_{12}), \quad (55)$$

$$c_{12} = c_{21} = \frac{1}{\lambda} \left[-\nu + \frac{g}{9} (2\tau_{11} - \tau_{22})(2\tau_{22} - \tau_{11}) \right], \quad (56)$$

$$c_{13} = c_{31} = \frac{1}{\lambda} \frac{g}{3} (2\tau_{11} - \tau_{22}) \tau_{12}, \quad (57)$$

$$c_{23} = c_{32} = \frac{1}{\lambda} \frac{g}{3} (2\tau_{22} - \tau_{11}) \tau_{12}, \quad (58)$$

$$d_1 = \frac{1}{2\lambda} F(\tau_e) (2\tau_{11} - \tau_{22}), \quad (59)$$

$$d_2 = \frac{1}{2\lambda} F(\tau_e) (2\tau_{22} - \tau_{11}), \quad (60)$$

$$j_2 = \tau_{11}^2 + \tau_{22}^2 - \tau_{11} \tau_{22} + 3\tau_{12}^2, \quad (61)$$

$$g = \begin{cases} \frac{9}{4j_2} \left(\frac{1}{e_t} - 1 \right) & \text{for } \dot{j}_2 \geq 0 \text{ and } j_2 = (j_2)_{\max}; \\ 0 & \text{for } \dot{j}_2 < 0 \text{ or } j_2 < (j_2)_{\max}, \end{cases} \quad (62)$$

$$\tau_e = j \frac{1}{2}, \quad (63)$$

$$F(\tau_e) = \frac{1}{\tau_c} \left(\frac{\tau_e}{\tau_c} \right)^{m-1}, \quad (64)$$

$$e_t = \left[1 + \frac{\nu}{\gamma} n_r \left(\frac{\tau_e}{\tau_0} \right)^{n_r-1} \right]^{-1}, \quad (65)$$

$$n_{ij} = \int_{-\eta/2}^{\eta/2} \tau_{ij} d\zeta, \quad (66)$$

$$m_{ij} = \int_{-\eta/2}^{\eta/2} \tau_{ij} \zeta d\zeta. \quad (67)$$

The edge of the spherical shell at $\theta = \theta_0$ is considered to be elastically supported. Hence the boundary condition at $\theta = \theta_0$ can be expressed as

$$\begin{bmatrix} \varphi_1(\theta_0) \\ u_1(\theta_0) \\ w(\theta_0) \\ u_2(\theta_0) \end{bmatrix} = \begin{bmatrix} a_{11} & a_{12} & a_{13} & a_{14} \\ a_{21} & a_{22} & a_{23} & a_{24} \\ a_{31} & a_{32} & a_{33} & a_{34} \\ a_{41} & a_{42} & a_{43} & a_{44} \end{bmatrix} \begin{bmatrix} n_{11}(\theta_0) \\ q_1(\theta_0) \\ m_{11}(\theta_0) \\ m_{12}(\theta_0) \end{bmatrix}, \quad (68)$$

where a_{ij} are the elastic constants of the support. At the apex $\theta = \pi$, all displacements and stresses must satisfy regularity conditions. The inelastic deformation of the shell will be determined by the governing equations, Eqs. (37-67), the boundary condition, Eq. (68), and the regularity conditions at $\theta = \pi$.

3. AXISYMMETRICAL DEFORMATION

When the magnitude of the external pressure is small, the deformation of the shell is axisymmetrical with respect to the polar axis. In this case, $\varphi_2 = \varphi = e_{12} = \kappa_{12} = n_{12} = q_2 = \tau_{12} = 0$ and all physical quantities are independent of β . We shall regard this axisymmetrical deformation as fundamental. In the following, we shall refer the quantities with a super bar to the fundamental deformation of the shell. The governing equations of the fundamental deformation are

$$\bar{\varphi}_1 = \lambda(\bar{u}_1 - \bar{w}_{,1}) , \quad (69)$$

$$\bar{\epsilon}_{11} = \bar{w} + \bar{u}_{1,1} + \frac{1}{2\lambda} \bar{\varphi}_1^2 , \quad (70)$$

$$\bar{\epsilon}_{22} = \bar{w} + \bar{u}_1 \cot \theta , \quad (71)$$

$$\bar{\kappa}_{11} = \bar{\varphi}_{1,1} , \quad (72)$$

$$\bar{\kappa}_{22} = \bar{\varphi}_1 \cot \theta , \quad (73)$$

$$\bar{n}_{11,1} + \bar{n}_{11} \cot \theta - \bar{n}_{22} \cot \theta + \bar{q}_1 - \bar{\varphi}_1 \bar{n}_{11} - p\bar{\varphi}_1 = 0 , \quad (74)$$

$$\begin{aligned} \bar{q}_{1,1} + \bar{q}_1 \cot \theta - (\bar{n}_{11} + \bar{n}_{22}) - (\bar{\varphi}_1 \bar{n}_{11})_{,1} \\ - \bar{\varphi}_1 \bar{n}_{11} \cot \theta - p = 0 , \end{aligned} \quad (75)$$

$$\bar{m}_{11,1} + \bar{m}_{11} \cot \theta - \bar{m}_{22} \cot \theta - \frac{1}{\lambda} \bar{q}_1 = 0 . \quad (76)$$

For axisymmetrical deformation, the shearing stress τ_{12} and shearing strain e_{12} vanish. Hence Eq. (52) can be written as

$$\dot{\tilde{\epsilon}} = \tilde{c} \dot{\tilde{\tau}} + \tilde{d} \quad (77)$$

where

$$\tilde{\epsilon} = \begin{bmatrix} \bar{\epsilon}_{11} \\ \bar{\epsilon}_{22} \end{bmatrix}, \quad \tilde{\tau} = \begin{bmatrix} \bar{\tau}_{11} \\ \bar{\tau}_{22} \end{bmatrix}, \quad \tilde{c} = \begin{bmatrix} c_{11} & c_{12} \\ c_{21} & c_{22} \end{bmatrix}, \quad \tilde{d} = \begin{bmatrix} d_1 \\ d_2 \end{bmatrix}, \quad (78)$$

where c_{ij} are calculated by Eqs. (53), (54) and (56) by setting $\tau_{ij} = \bar{\tau}_{ij}$. The inverse relation of Eq. (77) is

$$\dot{\tilde{\tau}} = \tilde{f} \dot{\tilde{\epsilon}} - \tilde{g}, \quad (79)$$

where

$$\tilde{f} = \tilde{c}^{-1} \quad \text{and} \quad \tilde{g} = \tilde{f} \tilde{d}.$$

$$\tilde{S} = \begin{bmatrix} \bar{n}_{11} \\ \bar{n}_{22} \\ \bar{m}_{11} \\ \bar{m}_{22} \end{bmatrix}, \quad \tilde{\epsilon} = \begin{bmatrix} \bar{\epsilon}_{11} \\ \bar{\epsilon}_{22} \\ \bar{\kappa}_{11} \\ \bar{\kappa}_{22} \end{bmatrix}. \quad (80)$$

By Eqs. (51), (66), (67), (79) and (80), we have

$$\dot{\tilde{S}} = \tilde{I} \dot{\tilde{\epsilon}} - \tilde{J}, \quad (81)$$

where \tilde{I} is a 4 x 4 matrix and \tilde{J} is a 4 x 1 matrix. The elements in \tilde{I} and \tilde{J} are

$$\begin{aligned}
I_{11} &= \int_{-\eta/2}^{\eta/2} f_{11} d\zeta, \quad I_{12} = I_{21} = \int_{-\eta/2}^{\eta/2} f_{12} d\zeta, \quad I_{22} = \int_{-\eta/2}^{\eta/2} f_{22} d\zeta, \\
I_{13} = I_{31} &= \int_{-\eta/2}^{\eta/2} f_{11} \zeta d\zeta, \quad I_{14} = I_{23} = I_{32} = I_{41} = \int_{-\eta/2}^{\eta/2} f_{12} \zeta d\zeta, \\
I_{24} = I_{42} &= \int_{-\eta/2}^{\eta/2} f_{22} \zeta d\zeta, \quad I_{33} = \int_{-\eta/2}^{\eta/2} f_{11} \zeta^2 d\zeta, \quad I_{34} = I_{43} = \int_{-\eta/2}^{\eta/2} f_{12} \zeta^2 d\zeta, \\
I_{44} &= \int_{-\eta/2}^{\eta/2} f_{22} \zeta^2 d\zeta, \quad J_1 = \int_{-\eta/2}^{\eta/2} g_1 d\zeta, \quad J_2 = \int_{-\eta/2}^{\eta/2} g_2 d\zeta, \quad J_3 = \int_{-\eta/2}^{\eta/2} g_1 \zeta d\zeta, \\
J_4 &= \int_{-\eta/2}^{\eta/2} g_2 \zeta d\zeta, \quad (82)
\end{aligned}$$

where f_{ij} and g_i are the elements in \underline{f} and \underline{g} . The inverse relation of Eq. (81) is

$$\dot{\underline{\xi}} = \underline{K} \dot{\underline{S}} + \underline{L}, \quad (83)$$

where

$$\underline{K} = \underline{I}^{-1}, \quad \underline{L} = \underline{K} \underline{J}. \quad (84)$$

By using Eq. (83), the incremental form of the field equations Eqs. (69-76) can be written as the following matrix equations:

$$\dot{\underline{U}} = \underline{A} \dot{\underline{U}} + \underline{B} \dot{\underline{V}} + \underline{C} \quad (85)$$

and

$$\underline{D} \dot{\underline{V}} - \underline{E} \dot{\underline{U}} + \underline{F} = 0, \quad (86)$$

where the prime represents the differentiation with respect to θ ,

$$\underline{U} = [\bar{\varphi}_1 \quad \bar{u}_1 \quad \bar{w} \quad \bar{n}_{11} \quad \bar{q}_1 \quad \bar{m}_{11}]^T \quad \text{and} \quad \underline{V} = [\bar{n}_{22} \quad \bar{m}_{22}]^T, \quad (87)$$

and the matrices \underline{A} , \underline{B} , \underline{C} , \underline{D} , \underline{E} and \underline{F} are given in Appendix A. After eliminating $\dot{\underline{v}}$ from Eq. (85) and (86), we obtain

$$\dot{\underline{u}}' = \underline{M} \dot{\underline{u}} + \underline{R}, \quad (88)$$

where

$$\underline{M} = \underline{A} + \underline{B} \underline{D}^{-1} \underline{E}, \quad (89)$$

and

$$\underline{R} = \underline{C} - \underline{B} \underline{D}^{-1} \underline{F}. \quad (90)$$

The boundary conditions at $\theta = \theta_0$ can be expressed as

$$\begin{bmatrix} \dot{\phi}_1(\theta_0) \\ \dot{u}_1(\theta_0) \\ \dot{w}(\theta_0) \end{bmatrix} = \begin{bmatrix} a_{11} & a_{12} & a_{13} \\ a_{21} & a_{21} & a_{23} \\ a_{31} & a_{32} & a_{33} \end{bmatrix} \begin{bmatrix} n_{11}(\theta_0) \\ q_1(\theta_0) \\ m_{11}(\theta_0) \end{bmatrix}. \quad (91)$$

At the apex, the boundary conditions are

$$\dot{\phi}_1(\pi) = \dot{u}(\pi) = \dot{q}(\pi) = 0. \quad (92)$$

In the following, we shall solve Eqs. (88), (91) and (92) by a modified Euler's method with a finite difference scheme.

Let n_m be an integer and $\Delta = (\pi - \theta_0)/n_m$, $\theta_i = \theta_0 + (i-1)\Delta$, ($i = 1, 2, \dots, n_m + 1$). $\underline{u}_i = \underline{u}(\theta_i)$, $\underline{M}_i = \underline{M}(\theta_i)$, $\underline{R}_i = \underline{R}(\theta_i)$. Eq. (88) can be expressed as

$$\dot{\underline{u}}_{i+1} = \dot{\underline{u}}_i + \frac{\Delta}{2} (\underline{M}_i \underline{u}_i + \underline{M}_{i+1} \dot{\underline{u}}_{i+1} + \underline{R}_i + \underline{R}_{i+1}), \quad (i=1, 2, \dots, n_m) \quad (93)$$

Let \underline{I}_0 be a unity matrix. Put

$$\tilde{V}_i = I_0 - \frac{\Delta}{2} M_i, \quad (94)$$

$$\tilde{W}_i = I_0 + \frac{\Delta}{2} M_i, \quad (95)$$

$$\tilde{Z}_i = \frac{\Delta}{2} (R_i + R_{i+1}), \quad (96)$$

$$P_i = \tilde{V}_{i+1}^{-1} \tilde{W}_i, \quad (97)$$

and

$$Q_i = \tilde{V}_{i+1}^{-1} \tilde{Z}_i. \quad (98)$$

Equation (93) can be written as

$$\dot{\tilde{U}}_{i+1} = P_i \dot{\tilde{U}}_i + Q_i. \quad (i = 1, 2, \dots, n_m) \quad (99)$$

Let

$$\dot{\tilde{U}}_i = \alpha_i \dot{\tilde{U}}_1 + \beta_i. \quad (100)$$

Hence

$$\alpha_1 = I_0 \text{ and } \beta_1 = 0. \quad (101)$$

By substitution, we obtain the following recurrence formula for determination of α_i and β_i .

$$\alpha_{i+1} = P_i \alpha_i \quad (102)$$

and

$$\beta_{i+1} = P_i \beta_i + Q_i. \quad (103)$$

At the apex, we have

$$\dot{\tilde{U}}_{n_m+1} = \alpha_{n_m+1} \dot{\tilde{U}}_1 + \beta_{n_m+1}. \quad (104)$$

Hence, by the boundary conditions, Eqs. (91) and (92), we have

$$\begin{array}{l}
 \dot{\underline{u}}_1 = \left[\begin{array}{l}
 a_{11} \dot{\bar{n}}_{11}(1) + a_{12} \dot{\bar{q}}_1(1) + a_{13} \dot{\bar{m}}_{11}(1) \\
 a_{21} \dot{\bar{n}}_{11}(1) + a_{22} \dot{\bar{q}}_1(1) + a_{23} \dot{\bar{m}}_{11}(1) \\
 a_{31} \dot{\bar{n}}_{11}(1) + a_{32} \dot{\bar{q}}_1(1) + a_{33} \dot{\bar{m}}_{11}(1) \\
 \dot{\bar{n}}_{11}(1) \\
 \dot{\bar{q}}_1(1) \\
 \dot{\bar{m}}_{11}(1)
 \end{array} \right] , \dot{\underline{u}}_{n_m+1} = \left[\begin{array}{l}
 \dot{\bar{w}}(n_m+1) \\
 \dot{\bar{n}}_{11}(n_m+1) \\
 0 \\
 \dot{\bar{m}}_{11}(n_m+1)
 \end{array} \right] .
 \end{array}
 \tag{105}$$

The first, second and fifth equations in Eq. (104) are the simultaneous equations for determination of $\dot{\bar{n}}_{11}(1)$, $\dot{\bar{q}}_1(1)$ and $\dot{\bar{m}}_{11}(1)$. After $\dot{\underline{u}}_1$ is calculated, $\dot{\underline{u}}_i (i = 2, 3, \dots, n_m + 1)$ can be determined by Eq. (100). To avoid the singularities involved in the matrices \underline{A} , \underline{B} , and \underline{E} at the apex, we consider that in the neighborhood of the apex, the shell is under a uniform contraction. Hence, at the apex, we have $\dot{\bar{n}}_{11}(\pi) = \dot{\bar{n}}_{22}(\pi)$, $\dot{\bar{m}}_{11}(\pi) = \dot{\bar{m}}_{22}(\pi)$ and $\dot{\bar{\varphi}}_1(\pi) = \dot{\bar{w}}(\pi) = \dot{\bar{n}}_{11}(\pi) = \dot{\bar{q}}_1(\pi) = \dot{\bar{m}}_1(\pi) = 0$. From these conditions, we can find the matrices $\underline{M}(\pi)$ and $\underline{R}(\pi)$.

Our calculation is based on an iterative procedure, i.e. in each incremental step, we assume a condition of either (i) loading or (ii) unloading or reloading and find the increments $\dot{\underline{u}}_i$ and $\dot{\underline{v}}_i$ for each spatial station. Then, we check the assumed condition. This iterative procedure continues until the calculated condition agrees with the assumed condition at each station of the shell.

It is found that the matrix involved in the evaluation of $\dot{\bar{n}}_{11}(1)$, $\dot{\bar{q}}_1(1)$ and $\dot{\bar{m}}_{1i}(1)$ is nearly singular. To improve the accuracy of our computation, the computing program is written in double precision. The inversion of a nearly singular matrix is carried out by an iterative procedure based on the residual derived from the approximate solution in each iterative step.

4. ASYMMETRICAL BIFURCATION

When the external pressure is large, the deformation of the shell may bifurcate from the fundamental axisymmetrical configuration to a shape with an asymmetrical mode. In the following, we shall employ Shanley's concept of inelastic bifurcation under increasing load [1] to analyze the asymmetrical bifurcation of the deep spherical shell. Shanley's concept was later elaborated on by Hill [3,4] based on the argument of uniqueness of solution incorporated with the comparison theorems of linear and nonlinear solids. Hill's conclusion can be stated as follows: During the incremental process of deformation of a solid body, if the constitutive relation is definite and independent of the situations of loading and unloading (or reloading), the relations between stress rates and strain rates are linear. In this case, the material is referred to as a linear solid and the potential function is a quadrate of the strain rate tensor with coefficients dependent on the state of stress. On the other hand, if the constitutive relations are dependent on the situation of loading and unloading, then the form of the potential function would depend on the strain rate tensor and hence the con-

stitutive relations are nonlinear. In this case, the material is referred to as a nonlinear solid. According to these definitions of linear and nonlinear solids it is seen that the potential function W_N for a nonlinear solid would coincide with the quadratic potential function W_L for the corresponding linear solid in a part of the strain rate space. In the region where $W_N \neq W_L$, we have $W_N > W_L$ for most materials. It can be shown by the comparison theorem that if the difference of potentials $W_N - W_L$ is a convex function of the strain rate tensor at every point of the solid body, then the eigenstate in the bifurcation of a nonlinear solid is reached at a higher bifurcation load in comparison with the bifurcation of a corresponding linear solid. Hence, the constitutive relations used for the analysis of bifurcation with the smallest initial load must be linear in the sense just described, i.e. the constitutive relations should be definite and independent of the mode of bifurcation. From the computational point of view, the moduli used for the incremental deformation due to bifurcation should be determined first and the bifurcation analysis is simply a check as to whether the bifurcated deformation is possible. Such a process is similar to what we use for the bifurcation analysis of elastic solids. Note that, under an increasing load, it would be proper to use the constitutive relations obtained from the incremental fundamental deformation of the solid body for the analysis of the critical condition of bifurcation.

In the bifurcation analysis, let us denote the additional displacement components introduced by bifurcation by \underline{u}_1 and \underline{w} , the

rotations by $\bar{\varphi}_i$ and φ , membrane strains by \bar{e}_{ij} , bending strains by $\underline{\kappa}_{ij}$, membrane forces by \bar{n}_{ij} , transverse shears by \bar{q}_i , moment resultants by \bar{m}_{ij} , etc. We have

$$\begin{aligned}
 u_1 &= \bar{u}_1 + \underline{u}_1, \quad u_2 = \underline{u}_2, \quad w = \bar{w} + \underline{w}, \\
 \varphi_1 &= \bar{\varphi}_1 + \underline{\varphi}_1, \quad \varphi_2 = \underline{\varphi}_2, \quad \varphi = \underline{\varphi}, \\
 \epsilon_{11} &= \bar{\epsilon}_{11} + \underline{\epsilon}_{11}, \quad \epsilon_{22} = \bar{\epsilon}_{22} + \underline{\epsilon}_{22}, \quad \epsilon_{12} = \underline{\epsilon}_{12}, \\
 \kappa_{11} &= \bar{\kappa}_{11} + \underline{\kappa}_{11}, \quad \kappa_{22} = \bar{\kappa}_{22} + \underline{\kappa}_{22}, \quad \kappa_{12} = \underline{\kappa}_{12}, \\
 n_{11} &= \bar{n}_{11} + \underline{n}_{11}, \quad n_{22} = \bar{n}_{22} + \underline{n}_{22}, \quad n_{12} = \underline{n}_{12}, \\
 q_1 &= \bar{q}_1 + \underline{q}_1, \quad q_2 = \underline{q}_2, \\
 m_{11} &= \bar{m}_{11} + \underline{m}_{11}, \quad m_{22} = \bar{m}_{22} + \underline{m}_{22}, \quad m_{12} = \underline{m}_{12}.
 \end{aligned} \tag{106}$$

Substituting Eq. (106) into Eqs. (37-50) and neglecting the second order terms of those quantities due to bifurcation, we obtain the governing linear equations for the eigenstate of bifurcation where the the critical load is involved implicitly in the nonlinear elastic pre-bifurcation deformation. In the following, we shall assume that φ is small and drop all terms involving φ in the field equations. To eliminate the β -dependence in the field equations, let

$$\begin{aligned}
 \underline{u}_1(\theta, \beta) &= u_1(\theta) \sin n\beta, \quad \underline{u}_2(\theta, \beta) = u_2(\theta) \cos n\beta, \quad \underline{w}(\theta, \beta) = w(\theta) \sin n\beta, \\
 \underline{\varphi}_1(\theta, \beta) &= \varphi_1(\theta) \sin n\beta, \quad \underline{\varphi}_2(\theta, \beta) = \varphi_2(\theta) \cos n\beta,
 \end{aligned}$$

$$\begin{aligned}
\underline{e}_{11}(\theta, \beta) &= e_{11}(\theta) \sin n\beta, & \underline{e}_{22}(\theta, \beta) &= e_{22}(\theta) \sin n\beta, \\
\underline{e}_{12}(\theta, \beta) &= e_{12}(\theta) \cos n\beta, \\
\underline{\kappa}_{11}(\theta, \beta) &= \kappa_{11}(\theta) \sin n\beta, & \underline{\kappa}_{22}(\theta, \beta) &= \kappa_{22}(\theta) \sin n\beta, \\
\underline{\kappa}_{12}(\theta, \beta) &= \kappa_{12}(\theta) \cos n\beta, & (107) \\
\underline{n}_{11}(\theta, \beta) &= n_{11}(\theta) \sin n\beta, & \underline{n}_{22}(\theta, \beta) &= n_{22}(\theta) \sin n\beta, \\
\underline{n}_{12}(\theta, \beta) &= n_{12}(\theta) \cos n\beta, \\
\underline{q}_1(\theta, \beta) &= q_1(\theta) \sin n\beta, & \underline{q}_2(\theta, \beta) &= q_2(\theta) \cos n\beta, \\
\underline{m}_{11}(\theta, \beta) &= m_{11}(\theta) \sin n\beta, & \underline{m}_{22}(\theta, \beta) &= m_{22}(\theta) \sin n\beta, \\
\underline{m}_{12}(\theta, \beta) &= m_{12}(\theta) \cos n\beta,
\end{aligned}$$

where n is an integer. The resulting field equations in our eigenvalue problem are

$$\varphi_1 = \lambda(u_1 - w_{,1}), \quad (108)$$

$$\varphi_2 = \lambda(u_2 - nw \csc \theta), \quad (109)$$

$$e_{11} = w + u_{1,1} + \frac{1}{\lambda} \bar{\varphi}_1 \varphi_1, \quad (110)$$

$$e_{22} = w + u_1 \cot \theta - nu_2 \csc \theta, \quad (111)$$

$$e_{12} = \frac{1}{2} (u_{2,1} + nu_1 \csc \theta - u_2 \cot \theta + \frac{1}{\lambda} \bar{\varphi}_1 \varphi_2), \quad (112)$$

$$\kappa_{11} = \varphi_{1,1}, \quad (113)$$

$$\kappa_{22} = -n\varphi_2 \csc \theta + \varphi_1 \cot \theta, \quad (114)$$

$$\kappa_{12} = \frac{1}{2} (\varphi_{2,1} + n\varphi_1 \csc \theta - \varphi_2 \cot \theta), \quad (115)$$

$$\begin{aligned}
n_{11,1} + n_{11} \cot \theta - nn_{12} \csc \theta - n_{22} \cot \theta + q_1 \\
- (\bar{\varphi}_1 n_{11} + \bar{n}_{11} \varphi_1) - p\varphi_1 = 0, \quad (116)
\end{aligned}$$

$$m_{22} + 2n_{12} \cot \theta + n_{12,1} \sin \theta + q_2 \sin \theta - (\bar{n}_{22}\omega_2 + \bar{\omega}_1 n_{12}) \sin \theta - p\omega_2 \sin \theta = 0, \quad (117)$$

$$q_{1,1} + q_1 \cot \theta - nq_2 \csc \theta - (n_{11} + n_{22}) - (\bar{\omega}_1 n_{11,1} + \bar{n}_{11,1} \omega_1 + \bar{\omega}_{1,1} n_{11} + \bar{n}_{11} \omega_{1,1}) - (\bar{\omega}_1 n_{11} + \bar{n}_{11} \omega_1) \cot \theta + (\bar{\omega}_1 n_{12} + \bar{n}_{22} \omega_2) n \csc \theta = 0, \quad (118)$$

$$m_{11,1} + m_{11} \cot \theta - nm_{12} \csc \theta - m_{22} \cot \theta - \frac{1}{\lambda} q_1 = 0, \quad (119)$$

$$nm_{22} \csc \theta + 2m_{12} \cot \theta + m_{12,1} - \frac{1}{\lambda} q_2 = 0. \quad (120)$$

Since the prebifurcation deformation is axisymmetrical, we can set $\tau_{ij} = \bar{\tau}_{ij}$ for $i, j \neq 1, 2$ and $\tau_{12} = 0$ in Eqs. (55), (57), (58) and (61) when we determine the material constants. Hence, if we denote

$$\underline{S} = \begin{bmatrix} n_{11} \\ n_{22} \\ m_{11} \\ m_{22} \end{bmatrix} \quad \text{and} \quad \underline{\xi} = \begin{bmatrix} \epsilon_{11} \\ \epsilon_{22} \\ \kappa_{11} \\ \kappa_{22} \end{bmatrix}, \quad (121)$$

then

$$\underline{\xi} = \underline{K} \underline{S}, \quad (122)$$

where \underline{K} is given by Eq. (84). The rest of the constitutive relations are

$$\epsilon_{12} = \bar{\kappa}_{11} n_{12} \quad (123)$$

and

$$\kappa_{12} = \bar{\kappa}_{22} m_{12}, \quad (124)$$

where

$$\bar{K}_{11} = \frac{1 + \nu}{\lambda \eta} \quad , \quad \bar{K}_{22} = \frac{12(1 + \nu)}{\lambda \eta^3} \quad , \quad (125)$$

Hence Eqs. (123) and (124) are elastic relations. Let

$$\tilde{U}^* = [\varphi_1 \ w \ u_1 \ u_2 \ q_1 \ n_{11} \ m_{11} \ m_{12}]^T \quad (126)$$

and

$$\tilde{V}^* = [\varphi_2 \ q_2 \ n_{22} \ m_{22} \ n_{12}]^T. \quad (127)$$

Our governing equations can be written as the following equations:

$$\tilde{U}^{*'} = \tilde{A}^* \tilde{U}^* + \tilde{B}^* \tilde{V}^* \quad (128)$$

and

$$\tilde{D}^* \tilde{V}^* + \tilde{E}^* \tilde{U}^* = 0. \quad (129)$$

The matrices \tilde{A}^* , \tilde{B}^* , \tilde{D}^* and \tilde{E}^* are given in Appendix B. After elimination of \tilde{V}^* from Eqs. (128) and (129), we have

$$\tilde{U}^{*'} = \tilde{M}^* \tilde{U}^* \quad , \quad (130)$$

where

$$\tilde{M}^* = \tilde{A}^* - \tilde{B}^* \tilde{D}^{*-1} \tilde{E}^* \quad . \quad (131)$$

Equation (130) can be expressed as the following difference equation:

$$\tilde{U}_{i+1}^* = \tilde{P}_i^* \tilde{U}_i^* \quad , \quad (132)$$

where

$$\tilde{P}_i^* = (\tilde{I}_0 - \frac{\Delta}{2} \tilde{M}_{i+1}^*)^{-1} (\tilde{I}_0 + \frac{\Delta}{2} \tilde{M}_i^*) \quad . \quad (133)$$

Thus, if we write

$$\underline{u}_1^* = \underline{\alpha}_1^* \underline{u}_1^* , \quad (134)$$

we have

$$\underline{\alpha}_1^* = \underline{I} \quad (135)$$

and

$$\underline{\alpha}_{i+1}^* = \underline{P}_i^* \underline{\alpha}_i^* . \quad (136)$$

Hence all $\underline{\alpha}_i^*$ ($i = 1, 2, \dots, n+1$) can be calculated. Intuitively, we know that when the configuration of the spherical shell is deep enough and the supporting edge is sufficiently rigid, bifurcation would not be governed by the case $n = 1$. The boundary conditions for cases $n \neq 1$ can be written as

$$\underline{u}_1^* = \begin{bmatrix} a_{11} n_{11}(\theta_0) + a_{12} q_1(\theta_0) + a_{13} m_{11}(\theta_0) + a_{14} m_{12}(\theta_0) \\ a_{31} n_{11}(\theta_0) + a_{32} q_1(\theta_0) + a_{33} m_{11}(\theta_0) + a_{34} m_{12}(\theta_0) \\ a_{21} n_{11}(\theta_0) + a_{22} q_1(\theta_0) + a_{23} m_{11}(\theta_0) + a_{24} m_{12}(\theta_0) \\ a_{41} n_{11}(\theta_0) + a_{42} q_1(\theta_0) + a_{43} m_{11}(\theta_0) + a_{44} m_{12}(\theta_0) \\ q_1(\theta_0) \\ n_{11}(\theta_0) \\ m_{11}(\theta_0) \\ m_{12}(\theta_0) \end{bmatrix} \quad (137)$$

and

$$\underline{u}_{n+1}^* = [0 \ 0 \ 0 \ 0 \ q_1(\pi) \ n_{11}(\pi) \ m_{11}(\pi) \ m_{12}(\pi)]^T . \quad (138)$$

Since

$$\underline{u}_{n+1}^* = \underline{\alpha}_{n+1}^* \underline{u}_1^* , \quad (139)$$

with a substitution of Eqs. (137) and (138) into Eq. (139), a characteristic equation can be obtained by setting the determinant derived from the coefficients of $n_{11}(\theta_0)$, $q_1(\theta_0)$, $m_{11}(\theta_0)$, $m_{12}(\theta_0)$ in the resulting first four equations zero. The critical pressure for bifurcation is then determined by the resulting characteristic equation. In our computation, at each incremental step, we check the value of the characteristic determinant. The critical pressure is determined from the determinant versus pressure curve for each value of n .

5. RESULTS AND DISCUSSIONS

In our numerical computations, we deal with a deep spherical shell whose geometry is similar to the hull of the ALVIN vehicle used for deep ocean exploration. The radius of the middle surface of the shell is 40 inches and the thickness is $h_0 = 1.93$ inches. The shell contains a hatch with polar angle $\theta_0 = 15^\circ$. The actual hull of the ALVIN vehicle also has three viewports. However in our shell model, the openings of viewports are neglected for simplicity of analysis. The shell is thickened in the vicinity of the hatch opening. We assume a linear variation in shell thickness in the region $15^\circ \leq \theta \leq 24^\circ$. At the edge of the hatch opening, the shell thickness is 3.6 inches. Although the computing program is written to include the general case of elastic support at the edge of the shell, in our computation, we only consider a special case of built-in edge for which $a_{ij} = 0$ ($i = 1,4$ and $j = 1,4$) in Eq. (68).

The material of the shell is 5AL 2Cb 1Ta - 0.8 Mo titanium alloy whose inelastic mechanical behavior can be represented with good accuracy by a Ramberg-Osgood stress-strain relation with $E = 16.5 \times 10^6$ psi, $\nu = 0.3$, $\sigma_0 = 17.0 \times 10^4$ psi, and $n_r = 50.8$. In our study, the effect of creep under high external pressure is also considered. Because of the lack of the creep data for titanium alloy under room temperature condition, we set $\sigma_c = 65.4 \times 10^4$ psi and $m = 9.9$ in the power law of steady creep in our calculation. A computing program is written in FORTRAN language for the IBM 370 computer. The list of the program is shown in Appendix C. The time interval used in our computation is so chosen that the difference in deflection of the shell is insignificant when we halve the time interval.

The shell is submerged into the sea water with a rate of 285 feet/minute (123.6 psi/min.) and then remains thereafter at a depth of 13,200 feet where the corresponding external pressure acting on the middle surface of the shell is $p = 0.00742$. When the magnitude of this external pressure is sufficiently small, the deformation of the shell is axisymmetrical. The average normal displacement, \bar{w}_{ave} is plotted against the time in Fig. 2 where the logarithmic scale is used for time. It is found that \bar{w}_{ave} increases as a linear function of time for $p < 0.00742$ and then remains at a constant value when $p = 0.00742$. For this pressure history, the effect of creep is not noticeable for $t < 10^5$ minutes.

In Figs. 3 and 4, the tangential component of displacement in the meridional direction \bar{u}_1 and the normal outward component of displacement \bar{w} are plotted as functions of θ for $p = 0.005194$ and $p = 0.007420$. It is found that in the region distant from the edge, the deformation of the shell is essentially the combination of a uniform contraction and a rigid body translation in the direction of the polar axis. Hence, near the apex, \bar{u}_1 and \bar{w} can be expressed approximately as

$$\bar{u}_1 = \gamma \sin \theta, \quad \bar{w} = \delta - \gamma \cos \theta, \quad (140)$$

where δ and γ are constants.

The membrane stresses \bar{n}_{11} and \bar{n}_{22} and the transverse shear \bar{q}_1 are plotted against θ in Figs. 6, 7 and 8. Stress concentration is found in \bar{n}_{11} and \bar{q}_1 at the clamped edge of the shell. Due to the junction of the uniform shell thickness and the variable shell thickness in the region close to the edge, the variation in \bar{n}_{22} is not smooth in the vicinity of $\theta = 24^\circ$. When the value of θ is sufficiently large, both \bar{n}_{11} and \bar{n}_{22} approach a value corresponding to the membrane stress in a uniformly contracted shell \bar{n}_{11} and $\bar{n}_{22} = p/2$ and the value of \bar{q}_1 approaches zero. The variation in \bar{m}_{11} and \bar{m}_{22} are shown in Figs. 8 and 9. Again, it is seen that both \bar{m}_{11} and \bar{m}_{22} approach zero when θ increases. From Figs. 5-9, it is found that in the region $65^\circ \leq \theta \leq 180^\circ$, the shell is under a uniform contraction. The effect of the clamped edge is only restricted to the region $\theta < 65^\circ$.

In order to study the effect of creep, the spherical hull is submerged to the depth 16,000 feet and 18,000 feet below the sea level. The corresponding pressures are $p = 0.00903$ and 0.01010 . For these pressures, the \bar{w}_{ave} versus t curves are shown in Fig. 2. It is found that the increment in the average normal deflection due to the steady creep is small. When $p = 0.01010$, it is nearly 3% for $t = 10^5$ minutes.

Next, we consider the case without creep in which the pressure can increase indefinitely. The pressure versus average normal displacement curve for axisymmetrical deformation is shown in Fig. 10. At $p = p_c = 0.02070$, equivalent to a depth of submergence of 35,000 feet, the p versus \bar{w}_{ave} curve reaches a maximum point which defines the ultimate load for axisymmetrical collapse of the shell. Note that this ultimate load for axisymmetrical collapse of the shell in the inelastic range is much smaller than the classical elastic buckling load of a complete spherical shell which is $(p)_{classical} = 2/[3(1-\nu^2)]^{3/2} = 1.225$. The critical load for yielding of a complete spherical shell is $(p)_{yielding} = 2\tau_0 = 0.0206$ which is very close to our p_c . In order to determine whether the shell may bifurcate before the ultimate load is reached, we employ the method described in Section 4 for the analysis of asymmetrical bifurcation with increasing load. It is found that asymmetrical bifurcation can occur at $p = p_b = 0.01916$ and $n = 2$. The critical depth of submergence for bifurcation is approximately 33,000 feet. As a result of asymmetrical bifurcation, the actual load-carrying capacity will be smaller than the one found based on the axisymmetrical deformation. In order

to determine the actual load-carrying-capacity of the shell, post bifurcation analysis must be considered. Note that the difference between p_c and p_D is small and we could anticipate that the actual load-carrying-capacity in the post-bifurcation stage would lie somewhere between these two values.

6. CONCLUDING REMARKS

The following conclusions can be drawn about the buckling of deep spherical shells in the inelastic range:

(1) When the magnitude of external pressure is sufficiently small; the deformation of the shell is axisymmetrical. Asymmetrical bifurcation occurs when the external pressure reaches a certain critical value.

(2) In the prebifurcation stage, the deformation of the shell in the region distant from the edge of the shell is a uniform contraction superposed on a rigid body translation in the direction of the polar axis. Stress concentration occurs in the vicinity of the edge.

(3) Under room temperature condition, the effect of creep is usually insignificant within the limit of time of operation.

(4) For the deep spherical shell fabricated of titanium alloy, asymmetrical bifurcation occurs when the inelastic deformation of the shell becomes prominent. The actual load-carrying-capacity of the shell after bifurcation is smaller than the limit load determined by the axisymmetrical deformation of the shell. However, the difference is found to be small.

7. REFERENCES

1. Shanley, F. R., "Inelastic Column Theory," Journal of the Aeronautical Sciences, 14, 1947, 261-267.
2. Sewell, M. J., "A Survey of Plastic Buckling," Study No. 6, Stability, Solid Mechanics Division, University of Waterloo, Waterloo, Ontario, Canada.
3. Hill, R., "A General Theory of Uniqueness and Stability in Elastic-Plastic Solids," J. Mech. and Phys. Solids, 6, 1958, 236-249.
4. Hill, R., "Bifurcation and Uniqueness in Nonlinear Mechanics of Continua," Prob. Cont. Mech., SIAM, 1961, 155-164.
5. Roth, R. S., "Plastic Buckling of Thin Shallow Spherical Shells," Proc. of the 4th U. S. Nat. Cong. of Appl. Mech. 1962, 1057-1065.
6. Hayes, J. C. and Lee, L. H. N., "Inelastic Buckling of Axisymmetrical Shells." J. Eng. Mech. Div. 96, 1970, 1107-1123.
7. Murphy, L. M. and Lee, L. H. N., "Inelastic Buckling Process of Axially Compressed Cylindrical Shells Subject to Edge Constraints," Int. J. Solids Structures 1, 1971, 1153-1170.
8. Huang, N. C., "Inelastic Buckling of Eccentrically Loaded Columns," Themis Report UND-73-3, University of Notre Dame, Notre Dame, Indiana, AIAA J. 11, 1973, 974-979.
9. Hutchinson, J. W., "On the Postbuckling Behavior of Imperfection-Sensitive Structures in the Elastic Range," J. Appl. Mech. 39, 1972, 155-162.
10. Leech, J. W., Witmer, E. A., and Pian, T. H. H., "Numerical

Calculation Technique for Large Elastic-Plastic Transient
Deformations of Thin Shells," AIAA J. 6, 1968, 2352-2359.

11. Sanders, J. L., Jr., "Nonlinear Theories for Thin Shells," Quart.
of Appl. Math. 21, 1963, 21-36.

APPENDIX A: MATRICES \underline{A} , \underline{B} , \underline{C} , \underline{D} , \underline{E} , and \underline{F}

The matrices \underline{A} , \underline{B} , \underline{C} , \underline{D} , \underline{E} and \underline{F} are given as follows:

$$\underline{A} = \begin{bmatrix} 0 & 0 & 0 & K_{31} & 0 & K_{33} \\ -\phi/\lambda & 0 & -1 & K_{11} & 0 & K_{13} \\ -1/\lambda & 1 & 0 & 0 & 0 & 0 \\ \bar{n}_{11} + p & 0 & 0 & \bar{\phi}_1 - \cot \theta & -1 & 0 \\ \bar{n}_{11} + \bar{n}_{11}(\bar{\phi}_1 + \cot \theta) & 0 & 0 & 1 + \bar{\phi}_1 + \bar{\phi}_1^2 + K_{31}\bar{n}_{11} & -\bar{\phi}_1 - \cot \theta & K_{33}\bar{n}_{11} \\ 0 & 0 & 0 & 0 & 1/\lambda & -\cot \theta \end{bmatrix}$$

$$\underline{B} = \begin{bmatrix} K_{32} & K_{34} \\ K_{12} & K_{14} \\ 0 & 0 \\ \cot \theta & 0 \\ 1 + \bar{\phi}_1 \cot \theta + K_{32}\bar{n}_{11} & K_{34}\bar{n}_{11} \\ 0 & \cot \theta \end{bmatrix}$$

$$\underline{C} = \begin{bmatrix} L_3 \\ L_1 \\ 0 \\ p\bar{\phi}_1 \\ p + L_3\bar{n}_{11} \\ 0 \end{bmatrix}$$

$$\underline{D} = \begin{bmatrix} K_{22} & K_{24} \\ K_{42} & K_{44} \end{bmatrix} ,$$

$$\underline{E} = \begin{bmatrix} 0 & \cot \theta & 1 & -K_{21} & 0 & -K_{23} \\ \cot \theta & 0 & 0 & -K_{41} & 0 & -K_{43} \end{bmatrix} ,$$

$$\underline{F} = \begin{bmatrix} L_2 \\ L_4 \end{bmatrix} .$$

APPENDIX B: MATRICES \underline{A}^* , \underline{B}^* , \underline{D}^* and \underline{E}^*

The nonvanishing elements in \underline{A}^* , \underline{B}^* , \underline{D}^* and \underline{E}^* are

$$a_{16}^* = K_{31} ,$$

$$a_{17}^* = K_{33} ,$$

$$a_{21}^* = -1/\lambda ,$$

$$a_{23}^* = 1 ,$$

$$a_{31}^* = -\bar{\varphi}_1/\lambda ,$$

$$a_{32}^* = -1 ,$$

$$a_{36}^* = K_{11} ,$$

$$a_{37}^* = K_{13} ,$$

$$a_{43}^* = -n \csc \theta ,$$

$$a_{44}^* = \cot \theta ,$$

$$a_{51}^* = \bar{n}_{11,1} + \bar{\varphi}_1(\bar{n}_{11} + p) + \bar{n}_{11} \cot \theta ,$$

$$a_{55}^* = -\bar{\varphi}_1 - \cot \theta ,$$

$$a_{56}^* = 1 + \bar{\varphi}_{1,1} + \bar{\varphi}_1^2 + K_{31}\bar{n}_{11} ,$$

$$a_{57}^* = K_{33} \bar{n}_{11} ,$$

$$a_{61}^* = \bar{n}_{11} + p ,$$

$$a_{65}^* = -1 ,$$

$$a_{66}^* = \bar{\varphi}_1 - \cot \theta ,$$

$$a_{75}^* = 1/\lambda ,$$

$$a_{77}^* = -\cot \theta ,$$

$$a_{78}^* = n \csc \theta$$

$$a_{88}^* = -2 \cot \theta ,$$

$$b_{13}^* = K_{32} ,$$

$$b_{14}^* = K_{34} ,$$

$$b_{33}^* = k_{12} ,$$

$$b_{34}^* = K_{14} ,$$

$$b_{41}^* = -\varphi_1/\lambda ,$$

$$b_{45}^* = 2\bar{K}_{11} ,$$

$$b_{51}^* = -n\bar{n}_{22} \csc \theta ,$$

$$b_{52}^* = n \csc \theta ,$$

$$b_{53}^* = 1 + \bar{\varphi}_1 \cot \theta + K_{32} \bar{n}_{11} ,$$

$$b_{54}^* = K_{34} \bar{n}_{11} ,$$

$$b_{63}^* = \cot \theta ,$$

$$b_{65}^* = n \csc \theta ,$$

$$b_{74}^* = \cot \theta ,$$

$$b_{82}^* = 1/\lambda ,$$

$$b_{84}^* = -n \csc \theta ,$$

$$d_{11}^* = -1 + \bar{\varphi}_{1,1} + 2\bar{\varphi}_1 \cot \theta - 2\lambda \bar{K}_{11} (\bar{n}_{22} + p) ,$$

$$d_{12}^* = 2(\bar{K}_{22}/\lambda + \lambda \bar{K}_{11}) ,$$

$$d_{13}^* = 2n[\lambda(\bar{K}_{11} + K_{12}) - K_{32}] \csc \theta ,$$

$$d_{14}^* = - 2n (K_{34} + \bar{K}_{22} - \lambda K_{14}) \csc \theta ,$$

$$d_{15}^* = -2\lambda\bar{K}_{11}(\bar{\phi}_1 - \cot \theta) - 2\lambda\bar{K}_{11,1} ,$$

$$d_{21}^* = 1 ,$$

$$d_{33}^* = K_{22} ,$$

$$d_{34}^* = K_{24} ,$$

$$d_{41}^* = n \csc \theta ,$$

$$d_{43}^* = K_{42} ,$$

$$d_{44}^* = K_{44} ,$$

$$d_{51}^* = \bar{\phi}_1 + \cot \theta ,$$

$$d_{55}^* = -2\lambda \bar{K}_{11} ,$$

$$e_{11}^* = n \csc \theta (2 \cot \theta - 3\bar{\phi}_1) ,$$

$$e_{12}^* = n \lambda \csc \theta (2 \cot^2 \theta - 1) ,$$

$$e_{13}^* = -2n \lambda \csc \theta \cot \theta ,$$

$$e_{14}^* = \lambda ,$$

$$e_{16}^* = 2n \csc \theta (\lambda K_{11} - K_{31}) ,$$

$$e_{17}^* = 2n \csc \theta (\lambda K_{13} - K_{33}) ,$$

$$e_{18}^* = 2 \bar{K}_{22} (\bar{\phi}_1 - \cot \theta) + 2\bar{K}_{22,1} ,$$

$$e_{22}^* = n \lambda \csc \theta ,$$

$$e_{24}^* = -\lambda ,$$

$$e_{32}^* = -1 ,$$

$$e_{33}^* = -\cot \theta ,$$

$$e_{34}^* = n \csc \theta ,$$

$$e_{36}^* = K_{21} ,$$

$$e_{37}^* = K_{23} ,$$

$$e_{41}^* = -\cot \theta ,$$

$$e_{46}^* = K_{41} ,$$

$$e_{47}^* = K_{43} ,$$

$$e_{51}^* = -2 n \csc \theta ,$$

$$e_{52}^* = -n \lambda \csc \theta \cot \theta ,$$

$$e_{53}^* = 2 n \lambda \csc \theta ,$$

$$e_{54}^* = -\lambda \cot \theta ,$$

$$e_{58}^* = 2 \bar{K}_{22} .$$

APPENDIX C: LIST OF COMPUTER PROGRAM

38

```

C THIS PROGRAM IS IN DOUBLE PRECISION. THIS IS INDICATED BY
C IMPLICIT REAL*8(A-H,O-Z)
C THE FOLLOWING IS THE INTEGRATION SUBROUTINE USED IN THIS PROGRAM
SUBROUTINE INT (V,DEL,N,VAL)
IMPLICIT REAL*8(A-H,O-Z)
DIMENSION V(51)
N1 = N-1
VAL = 0.0
DO 201 I = 1,N1,2
VAL = VAL + V(I) + 4.0 * V(I + 1) + V(I+2)
201 CONTINUE
VAL=VAL * DEL / 3.0
RETURN
END
C THE FOLLOWING IS THE DIFFERENTIATION SUBROUTINE
SUBROUTINE SLOP (V,DEL,N,VS)
IMPLICIT REAL*8(A-H,O-Z)
DIMENSION V(51),VS(51)
DD = 0.5 /DEL
DO 208 I = 2,N
VS(I) = DD*(V(I+1) - V(I-1))
208 CONTINUE
VS(1) = DD * ( -3.0 * V(1) + 4.0 * V(2) - V(3))
VS(N + 1) = DD *(3.0 * V(N + 1) - 4.0 * V(N) + V(N -1))
RETURN
END
C THE MATRIX ADDITION SUBROUTINE FOLLOWS
SUBROUTINE DMADD(A,B,R,N,M)
IMPLICIT REAL*8(A-H,O-Z)
DIMENSION A(1),B(1),R(1)
NM = N*M
DO 10 I = 1,NM
10 R(I) = A(I) + B(I)
RETURN
END
C THE MATRIX MULTIPLICATION SUBROUTINE FOLLOWS
SUBROUTINE DMPRD(A,B,R,N,M,L)
IMPLICIT REAL*8(A-H,O-Z)
DIMENSION A(1),B(1),R(1)
IR = 0
IK = -M
DO 10 K = 1,L
IK = IK + M
DO 10 J = 1,N
IR = IR + 1
JI = J-N
IB = IK
R(IR) = 0
DO 10 I = 1,M
JI = JI + N
IB = IB + 1
10 R(IR) = R(IR) + A(JI)*B(IB)
RETURN
END
IMPLICIT REAL*8(A-H,O-Z)
DIMENSION TH(51),T(51),CT(51),PH(51),U(51),W(51),XNTH(51),
1 XNPH(51),Q(51),XMTH(51),XMPH(51),TUTH(51,21),TUPH(51,21)
DIMENSION D1(51,21)
DIMENSION D2(51,21),G(51,21),GS(51,21),C(2,2),LA(2),MA(2),DD(2),
1 GA(2),FJ(2,2,21),GJ(2,21),X11(21),X12(21),X22(21),X13(21),X14(21)
DIMENSION X24(21),X33(21),X34(21),X44(21),Y1(21),Y2(21),Y3(21),
1 Y4(21),THPH(51,21),PHTH(51,21),TUTHD(51,21),TUPHD(51,21),CC(6)
DIMENSION AI(4,4),AJ(4),LB(4),MB(4),AL(4),AM(6,6),BM(6,2),CM(6),
1 XNTHP(51),PHP(51),DM(2,2),EM(2,6),FM(2),DE(2,6),BDE(6,6)
DIMENSION DEI(2,6,51),BDFK(6),BET(6),YMK(6,6),R(6,51),ALP(6,6)
1,DF(2),UNM(6,6),VM(6,6),WM(6,6,51),ZM(6,51),LC(6),MC(6),ZZ(6)
DIMENSION WW(6,6),VW(6,6),VZ(6),GBD(3),ANE(6,6),
1UMD(6,51),UND(6),LD(3),MD(3),VWR(6),BNE(6),DAL(3),GAD(3),ALPC(6)
DIMENSION TR(3,3),SD(4),ALI(4,51),ALI(4,4,51),ASD(4),X11(51,21),
1X12(51,21),X22(51,21),Y1(51,21),Y2(51,21),GSS(51,21),CK(51)
DIMENSION XSI(51,21),DFI(2,51),ESD(4),VMM(6,6,51),VD(2),VDI(2,51)
1,XJ2D(51,21),DELL(51),CWK(51),BETI(6,51),ALPI(6,6,51),GAM(3,3)
DIMENSION DBL(3),XO(3),YO(3),GBM(3,3),CPI(20),XJM(51,21),XJ2(51,21)
DIMENSION AKB(2,2,51),AKB(51),AKBP(51),AMS(8,8),BMS(8,5),DMS(5,5)
1,CS(50),AKCP(51),EMS(5,8),UNNM(8,8),AKC(51)
DIMENSION DES(5,8),BDES(8,8),LAS(5),MAS(5),YMK(8,8),ALPS(8,8),
1 WMS(8,8,51),LCS(8),MCS(8),VMMS(8,8,51),ALPIS(8,8,51),MWS(8,8)
DIMENSION VMS(8,8),VMSI(8,8),ANES(8,8),GAMS(4,4),MGAS1(4),MGAS2(4)

```

```

C THE FOLLOWING PARAMETERS TO BE READ IN ARE DEFINED HERE
C THO = HALF ANGLE OF HATCH, M = NUMBER OF INTERVALS THROUGH THICKNESS,
C N = NUMBER OF INTERVALS ON THE MERIDIONAL, NB = NUMBER OF INTERVALS
C IN WHICH THE THICKNESS VARIES NEAR THE HATCH, HO IS THE RELATIVE
C THICKNESS AT THE HATCH EDGE, TO = THE TIME AT WHICH THE PRESSURE
C BECOMES CONSTANT, PO = VALUE OF PRESSURE AT THIS POINT, XNU = POISSON'S
C RATIO, TUC = NONDIMENSIONALIZED STRESS CONSTANT IN THE CREEP RELATION,
C TUC = NONDIMENSIONALIZED STRESS CONSTANT IN THE RAMBERG-OSGOOD EQUATION,
C SM AND SN ARE EXPONENTS IN THE CREEP AND RAMBERG-OSGOOD EQUATIONS
C RESPECTIVELY, XLA = RATIO OF SHELL THICKNESS TO MID-SURFACE RADIUS,
C TD = TIME INCREMENT, TF = FINAL TIME
C THE FOLLOWING ARE PROGRAM CONTROL PARAMETERS
C IND = 0 FOR NO CREEP = 1 FOR CREEP, IF IP IS POSITIVE, VALUES OF U, W, PH,
C Q, XNTH, XNPH, XMTH, XMPH AND TH ARE PRINTED AT EACH TIME INCREMENT FOR
C EACH STATION ON THE MERIDIONAL. IF IP IS ZERO THESE ARE NOT PRINTED.
C 100 READ (5,*) THO, M, N, NB, HO, TO, PO, XNU, TUC, TUO, SM, SN, XLA, DT, TF, IND, IP
C IF KIP = 1 BIFURCATION IS CONSIDERED. IF 0 IT IS NOT, NII DENOTES
C FIRST VALUE OF THE BIFURCATION MODE PARAMETER NIF THE LAST, NINC IS
C THE INCREMENT. NBIFUR DENOTES THE NUMBER OF TIME INCREMENTS WHICH
C PASS PRIOR TO CHECKING FOR BIFURCATION
C READ(5,*) KIP, NII, NIF, NBIFUR, NINC
C AIJ ARE THE ELASTIC SUPPORT CONSTANTS
C READ (5,*) A11, A12, A13, A14, A21, A22, A23, A24, A31, A32, A33, A34, A41,
C 1 A42, A43, A44
C IF (M) 101, 500, 101
101 WRITE (6,8) THO, M, N, NB, HO, TO, PO, XNU
8 FORMAT (1X, 7H THETAO=E13.5, 1X, 2HM=13, 1X, 2HN=13, 1X, 3HNB=13, 1X,
1 3HHO=E13.5, 1X, 3HTO=E13.5, 1X, 3HPO=E13.5, 1X, 3HNU=E13.5)
WRITE (6,9) TUC, TUO, SM, SN, XLA, DT
9 FORMAT (1X, 4HTUC=E13.5, 1X, 4HTUO=E13.5, 1X, 3HMS=E13.5, 1X, 3HNS=E13.5
1, 1X, 7HLAMBDA=E13.5, 1X, 7HDELTA=E13.5)
WRITE (6, 2551) TF, IND, IP, KIP, NII, NIF, NBIFUR, NINC
2551 FORMAT (1X, 3HTF=E13.5, 1X, 6HINDEX=13, 1X, 3HIP=13, 1X, 4HKIP=13, 2X,
1 4HNII=13, 1X, 4HNIF=13, 2X, 7HNBIFUR=13, 2X, 5HNINC=13)
WRITE (6, 1449)
1449 FORMAT (2X, 32HELASTIC SUPPORT CONSTANTS A(I,J))
WRITE (6, 1550) A11, A12, A13, A14
WRITE (6, 1550) A21, A22, A23, A24
WRITE (6, 1550) A31, A32, A33, A34
WRITE (6, 1550) A41, A42, A43, A44
1550 FORMAT (1X, 4E13.5)
FIND = IND
XLB = 1.0/XLA
SF33=XLA/(1.0+XNU)
XN = N
XM = M
TAX = 3.141592654 - THO
DEL = TAX/XN
N1 = N + 1
N2 = N + 2
NB1 = NB + 1
M1 = M + 1
DTT=DT
FNB=NB
HH=(HO-1.0)/FNB
TIM = 0.0
P = 0.0
PR = PO/TO
PRS=0.01*PR*PR
WAVE = 0.0
NT = 0
XNN=TO/DT+0.01
NN = XNN
TUCM = TUC**SM
SM1 = SM - 1.0
SN1 = SN - 1.0
CO=3.0*SN/7.0
DEL2 = 0.5*DEL
DO 38 I = 1,6
R(I, N1) = 0.0
CM(I) = 0.0
BET(I, 1) = 0.0
DO 37 J = 1,6
AM(I, J) = 0.0
ALPI(I, J, 1) = 0.0
UNMI(I, J) = 0.0
37 CONTINUE
38 CONTINUE

```

```

DO 371 I=1,6
UNM(I,I)=1.0
ALP(I,I,1)=1.0
371 CONTINUE
DO 32 J=1,2
DFI(J,N1)=0.0
DO 33 I=1,6
BM(I,J)=0.0
DEI(J,I,N1)=0.0
33 CONTINUE
32 CONTINUE
DO 1502 I=1,8
DO 1500 J=1,8
AMS(I,J)=0.0
ALPIS(I,J,1)=0.0
UNNM(I,J)=0.0
1500 CONTINUE
DO 1501 J=1,5
BMS(I,J)=0.0
EMS(J,I)=0.0
1501 CONTINUE
1502 CONTINUE
DO 1506 I=1,8
UNN(I,I)=1.0
ALPIS(I,I,1)=1.0
1506 CONTINUE
DEI(1,4,N1)=1.0
DEI(2,6,N1)=1.0
AM(2,3)=-1.0
AM(3,1)=-XLB
AM(3,2)=1.0
AM(4,5)=-1.0
AM(6,5)=XLB
EM(1,1)=0.0
EM(1,3)=1.0
EM(1,5)=0.0
EM(2,2)=0.0
EM(2,3)=0.0
EM(2,5)=0.0
AMS(2,1)=-XLB
AMS(2,3)=1.0
AMS(3,2)=-1.0
AMS(6,5)=-1.0
AMS(7,5)=XLB
BMS(8,2)=XLB
EMS(1,4)=XLA
EMS(2,4)=-XLA
EMS(3,2)=-1.0
DO 14 I=1,N1
I1=I-1
X11=I1
TH(I)=TH0+X11*DEL
IF (I-NB1) 10,10,11
10 T(I)=H0-HH*X11
GO TO 12
11 T(I)=1.0
12 DELL(I)=T(I)/XM
AKBI(1,1,I)=1.0/(SF33*T(I))
AKBI(1,2,I)=0.0
AKBI(2,1,I)=0.0
AKBI(2,2,I)=12.0/(AKBI(1,1,I)*T(I)*T(I))
DO 13 J=1,M1
XJ=J
XSI(I,J)=-0.5*T(I)+(XJ-1.0)*DELL(I)
TUTH(I,J)=0.0
TUPH(I,J)=0.0
TUTHD(I,J)=0.0
TUPHD(I,J)=0.0
G(I,J)=0.0
GS(I,J)=0.0
GSS(I,J)=0.0
XJM(I,J)=0.0
13 CONTINUE
14 CONTINUE
DO 7341 I=1,N
SII=OSIN(TH(I))
CCO=DCOS(TH(I))
CS(I)=1.0/SII

```

```

7941 CT(I)=CCO/SII
DO 7890 I = 1,N2
PH(I) = 0.0
U(I) = 0.0
W(I) = 0.0
XNTH(I) = 0.0
XMPH(I) = 0.0
Q(I) = 0.0
XMTH(I) = 0.0
XMPH(I) = 0.0
7890 CONTINUE
403 WRITE (6,13) TIM,P,WAVE
15 FORMAT (1X,5HTIME=E13.5,1X,2HP=E13.5,1X,5HWAVE=E13.5)
IF(IP)240,240,16
16 WRITE(6,7749)
7749 FORMAT(' TH(I)=')
WRITE(6,18)(TH(I),I=1,N1)
WRITE (6,17)
17 FORMAT (1X,4HU(I))
WRITE (6,18) (U(I),I = 1,N1)
18 FORMAT (1X,8E14.5)
WRITE (6,19)
19 FORMAT (1X,4HW(I))
WRITE (6,18) (W(I),I = 1,N1)
WRITE(6,7704)
7704 FORMAT(' PH(I) =')
WRITE(6,18) (PH(I),I=1,N1)
WRITE(6,7701)
7701 FORMAT (' Q(I) = ')
WRITE(6,18) (Q(I),I=1,N1)
WRITE(6,7702)
7702 FORMAT(' XNTH(I) = ')
WRITE(6,18) (XNTH(I),I=1,N1)
WRITE(6,7711)
7711 FORMAT(' XNPH(I) = ')
WRITE(6,18) (XNPH(I),I=1,N1)
WRITE(6,7703)
7703 FORMAT(' XMTH(I) = ')
WRITE(6,18) (XMTH(I),I=1,N1)
WRITE(6,7706)
7706 FORMAT(' XMPH(I) = ')
WRITE(6,18) (XMPH(I),I=1,N1)
240 NT = NT + 1
TIM=TIM+DT
IF (TIM - TF) 411,411,100.
411 IF (NT-NN) 20,278,21
278 DT = 5.0*DTT
20 DP = PR*DTT
GO TO 22
21 DP = 0.0
DT=2.0*DT
22 PST = P
P = P + DP
PDOT = DP/DT
ITER = 1
CALL SLOP (XNTH,DEL,N,XNTHP)
CALL SLOP (PH,DEL,N,PHP)
DO 24 I = 1,N1
DO 23 J = 1,M1
XJ2(I,J) = TUTH(I,J)*(TUTH(I,J)-TUPH(I,J))+TUPH(I,J)*TUPH(I,J)
XJM(I,J) = DMAX1(XJM(I,J),XJ2(I,J))
TUE = DSQRT(XJ2(I,J))
ETA=CQ*(TUE/TUO)**SN1
THPH(I,J) = 2.0*TUTH(I,J) - TUPH(I,J)
PHTH(I,J) = 2.0*TUPH(I,J) - TUTH(I,J)
XLAF = 0.5*F/XLA
D1(I,J) = XLAF*THPH(I,J)*FIND
D2(I,J) = XLAF*PHTH(I,J)*FIND
IF (NT-1) 535,535,536
535 GSS(I,J)=0.0
GO TO 23
536 GSS(I,J) = 2.25*ETA/XJ2(I,J)
23 CONTINUE
24 CONTINUE
25 DO 36 I=1,N1
DELT = DELL(I)
DO 28 J = 1,M1

```

```

G(I,J) = GS(I,J)
C(1,1) = XLB*(1.0+G(I,J)*THPH(I,J)*THPH(I,J)/9.0)
C(1,2) = XLB*(-XNU + G(I,J)*THPH(I,J)*PHTH(I,J)/9.0)
C(2,1) = C(1,2)
C(2,2) = XLB*(1.0 + G(I,J)*PHTH(I,J)*PHTH(I,J)/9.0)
C DMINV IS THE DOUBLE PRECISION MATRIX INVERSION SUBROUTINE
CALL DMINV(C,2,DET,IA,MA)
DD(1) = D1(I,J)
DD(2) = D2(I,J)
CALL DMPRD(C,DD,GA,2,2,1)
DO 27 J1 = 1,2
DO 26 J2 = 1,2
FJ(J1,J2,J) = C(J1,J2)
26 CONTINUE
GJ(J1,J) = GA(J1)
27 CONTINUE
28 CONTINUE
DO 29 J = 1,M1
X11(J) = FJ(1,1,J)
X111(I,J) = X11(J)
X12(J) = FJ(1,2,J)
X121(I,J) = X12(J)
X22(J) = FJ(2,2,J)
X221(I,J) = X22(J)
X13(J) = FJ(1,1,J)*XSI(I,J)
X14(J) = FJ(1,2,J)*XSI(I,J)
X24(J) = FJ(2,2,J)*XSI(I,J)
X33(J) = X13(J)*XSI(I,J)
X34(J) = X14(J)*XSI(I,J)
X44(J) = X24(J)*XSI(I,J)
Y1(J) = GJ(1,J)
Y11(I,J) = Y1(J)
Y2(J) = GJ(2,J)
Y21(I,J) = Y2(J)
Y3(J) = GJ(1,J)*XSI(I,J)
Y4(J) = GJ(2,J)*XSI(I,J)
29 CONTINUE
CALL INT (X11,DELT,M,AI(1,1))
CALL INT (X12,DELT,M,AI(1,2))
AI(2,1) = AI(1,2)
CALL INT (X22,DELT,M,AI(2,2))
CALL INT (X13,DELT,M,AI(1,3))
AI(3,1) = AI(1,3)
CALL INT (X14,DELT,M,AI(1,4))
AI(2,3) = AI(1,4)
AI(3,2) = AI(1,4)
AI(4,1) = AI(3,2)
CALL INT (X24,DELT,M,AI(2,4))
AI(4,2) = AI(2,4)
CALL INT (X33,DELT,M,AI(3,3))
CALL INT (X34,DELT,M,AI(3,4))
AI(4,3) = AI(3,4)
CALL INT (X44,DELT,M,AI(4,4))
CALL INT (Y1,DELT,M,AJ(1))
CALL INT (Y2,DELT,M,AJ(2))
CALL INT (Y3,DELT,M,AJ(3))
CALL INT (Y4,DELT,M,AJ(4))
CALL DMINV (AI,4,DET,LB,MB)
CALL DMPRD (AI,AJ,AL,4,4,1)
DO 300 I1 = 1,4
ALI(I1,I) = AL(I1)
DO 301 I2 = 1,4
AII(I1,I2,I) = AI(I1,I2)
301 CONTINUE
300 CONTINUE
IF(I-NI)366,367,36
367 DO 565 I1=1,6
DO 564 I2=1,6
YMK(I1,I2)=0.0
564 CONTINUE
565 CONTINUE
YMK(2,3)=-1.0
YMK(2,4)=AI(1,1)+AI(1,2)
YMK(2,6)=AI(1,3)+AI(1,4)
R(2,N1)=AL(1)
GO TO 566
366 AM(1,4) = AI(3,1)
AM(1,6) = AI(3,3)

```

```

AM(2,1) = -PH(I)/XLA
AM(2,4) = AI(1,1)
AM(2,6) = AI(1,3)
COP = DCOS(PH(I))
AM(4,1) = XNTH(I) + PST*COP
AM(4,4) = PH(I) - CT(I)
SP = DSIN(PH(I))
AM(5,1) = XNTHP(I) + XNTH(I)*(PH(I) + CT(I)) -
1 PST*(SP - PH(I)*COP)
AM(5,4) = 1.0 + PHP(I) + PH(I)*PH(I) + AI(3,1)*XNTH(I)
AM(5,5) = -PH(I) - CT(I)
AM(5,6) = AI(3,3)*XNTH(I)
AM(6,6) = -CT(I)
BM(1,1) = AI(3,2)
BM(1,2) = AI(3,4)
BM(2,1) = AI(1,2)
BM(2,2) = AI(1,4)
BM(4,1) = CT(I)
BM(5,1) = 1.0 + PH(I)*CT(I) + AI(3,2)*XNTH(I)
BM(5,2) = AI(3,4)*XNTH(I)
BM(6,2) = CT(I)
CM(1) = AL(3)
CM(2) = AL(1)
CM(4) = PDOT*SP
CM(5) = PDOT*COP + AL(3) * XNTH(I) + PH(I)*PDOT*SP
DM(1,1) = AI(2,2)
DM(1,2) = AI(2,4)
DM(2,1) = AI(4,2)
DM(2,2) = AI(4,4)
EM(1,2) = CT(I)
EM(1,4) = -AI(2,1)
EM(1,6) = -AI(2,3)
EM(2,1) = CT(I)
EM(2,4) = -AI(4,1)
EM(2,6) = -AI(4,3)
FM(1) = AL(2)
FM(2) = AL(4)
CALL DMINV (DM,2,DET,LA,MA)
CALL DMPRD(DM,EM,DE,2,2,6)
CALL DMPRD(BM,DE,BDE,6,2,6)
CALL DMPRD(DM,FM,DF,2,2,1)
CALL DMPRD(BM,DF,BDF,6,2,1)
CALL DMADD(AM,BDE,YMK,6,6)
DO 35 I1 = 1,6
R(I1,1) = CM(I1) - BDFK(I1)
35 CONTINUE
DO 203 I1 = 1,2
DFI(I1,1) = DF(I1)
DO 202 I2 = 1,6
DEI(I1,I2,1) = DE(I1,I2)
202 CONTINUE
203 CONTINUE
566 DO 40 I1 = 1,6
DO 39 I2 = 1,6
DELY=DEL2*YMK(I1,I2)
VM(I1,I2) = UNM(I1,I2) - DELY
WM(I1,I2,1) = UNM(I1,I2) + DELY
39 CONTINUE
40 CONTINUE
CALL DMINV (VM,6,DET,LC,MC)
DO 42 I1 = 1,6
DO 41 I2 = 1,6
VMM(I1,I2,1) = VM(I1,I2)
41 CONTINUE
42 CONTINUE
36 CONTINUE
DO 45 I = 1,N
DO 44 I1 = 1,6
ZM(I1,I) = DEL2*(R(I1,I) + R(I1,I + 1))
44 CONTINUE
45 CONTINUE
DO 50 I = 1,N
IA=I+1
DO 46 I1 = 1,6
BET(I1)=BETI(I1,I)
ZZ(I1) = ZM(I1,I)
DO 47 I2 = 1,6
ALP(I1,I2)=ALPI(I1,I2,I)

```

```

NW(I1,I2) = WM(I1,I2,I)
VM(I1,I2) = VMM(I1,I2,IA)
47 CONTINUE
46 CONTINUE
CALL DMPRD(VM,WM,VW,6,6,6)
CALL DMPRD(VM,ZZ,VZ,6,6,1)
CALL DMPRD(VW,ALP,ANE,6,6,6)
CALL DMPRD(VW,BET,VWB,6,6,1)
DO 54 I1=1,6
BETI(I1,IA)=VWB(I1)+VZ(I1)
DO 53 I2=1,6
ALPI(I1,I2,IA)=ANE(I1,I2)
53 CONTINUE
54 CONTINUE
50 CONTINUE
XO(1) = 0.0
XO(2) = 0.0
XO(3) = 0.0
IT=1
GAM(1,1)=ALPI(1,4,N1)+A11*ALPI(1,1,N1)+A21*ALPI(1,2,N1)+A31*ALPI(1,3,N1)
GAM(1,2)=ALPI(1,5,N1)+A12*ALPI(1,1,N1)+A22*ALPI(1,2,N1)+A32*ALPI(1,3,N1)
GAM(1,3)=ALPI(1,6,N1)+A13*ALPI(1,1,N1)+A23*ALPI(1,2,N1)+A33*ALPI(1,3,N1)
GAM(2,1)=ALPI(2,4,N1)+A11*ALPI(2,1,N1)+A21*ALPI(2,2,N1)+A31*ALPI(2,3,N1)
GAM(2,2)=ALPI(2,5,N1)+A12*ALPI(2,1,N1)+A22*ALPI(2,2,N1)+A32*ALPI(2,3,N1)
GAM(2,3)=ALPI(2,6,N1)+A13*ALPI(2,1,N1)+A23*ALPI(2,2,N1)+A33*ALPI(2,3,N1)
GAM(3,1)=ALPI(3,4,N1)+A11*ALPI(3,1,N1)+A21*ALPI(3,2,N1)+A31*ALPI(3,3,N1)
GAM(3,2)=ALPI(3,5,N1)+A12*ALPI(3,1,N1)+A22*ALPI(3,2,N1)+A32*ALPI(3,3,N1)
GAM(3,3)=ALPI(3,6,N1)+A13*ALPI(3,1,N1)+A23*ALPI(3,2,N1)+A33*ALPI(3,3,N1)
DAL(1)=BETI(1,N1)
DAL(2)=BETI(2,N1)
DAL(3)=BETI(3,N1)
DO 91 I1=1,3
DO 90 I2=1,3
GBM(I1,I2) = GAM(I1,I2)
90 CONTINUE
91 CONTINUE
CALL DMINV (GAM,3,DET,LD,MD)
CALL DMPRD (GAM,DAL,GAD,3,3,1)
735 XO(1) = XO(1) - GAD(1)
XO(2) = XO(2) - GAD(2)
XO(3) = XO(3) - GAD(3)
CALL DMPPD(GBM,XO,YO,3,3,1)
DBL(1) = YO(1) + DAL(1)
DBL(2) = YO(2) + DAL(2)
DBL(3) = YO(3) + DAL(3)
AAA = DMAXI(DABS(DBL(1)),DABS(DBL(2)),DABS(DBL(3)))
IF(AAA- 0.00001) 798,798,799
799 IT = IT + 1
IF(IT - 10) 732,732,733
733 WRITE (6,734) IT
734 FORMAT(IX,3HIT=I3)
GO TO 500
732 CALL DMPRD(GAM,DBL,GAD,3,3,1)
GO TO 735
798 UMD(1,1) = A11*XO(1) + A12*XO(2) + A13*XO(3)
UMD(2,1) = A21*XO(1) + A22*XO(2) + A23*XO(3)
UMD(3,1) = A31*XO(1) + A32*XO(2) + A33*XO(3)
UMD(4,1)=XO(1)
UMD(5,1)=XO(2)
UMD(6,1)=XO(3)
DO 788 I1 = 1,6
CC(I1)= UMD(I1,1)
788 CONTINUE
DO 59 I=2,N1
DO 57 I1=1,6
DO 56 I2=1,6
ALP(I1,I2)=ALPI(I1,I2,I)
56 CONTINUE
57 CONTINUE

```



```

CALL DMPRD (ALP,CC,ALPC,6,6,1)
DO 58 I1=1,6
UMD(I1,I)=ALPC(I1)+BETI(I1,I)
58 CONTINUE
59 CONTINUE
DIF=0.0
DED = 0.0
DO 77 I = 1,N1
CK(I) = 0.0
CWK(I) = 0.0
DO 67 I2 = 1,6
UND(I2) = UMD(I2,I)
DO 66 I1 = 1,2
DE(I1,I2)=DEI(I1,I2,I)
66 CONTINUE
67 CONTINUE
DO 68 I1 = 1,2
DF(I1) = DFI(I1,I)
68 CONTINUE
CALL DMPRD (DE,UND,VD,2,6,1)
SD(2) = VD(1) - DF(1)
SD(4) = VD(2) - DF(2)
VDI(1,I) = SD(2)
VDI(2,I) = SD(4)
SD(1) = UND(4)
SD(3) = UND(6)
DO 70 I1 = 1,4
DO 69 I2 = 1,4
AI(I1,I2) = AII(I1,I2,I)
69 CONTINUE
70 CONTINUE
CALL DMPRD (AI,SD,ASD,4,4,1)
DO 71 I1 = 1,4
ESD(I1) = ASD(I1) + ALI(I1,I)
71 CONTINUE
DO 76 J = 1,M1
PX = ESD(1) + XSI(I,J) * ESD(3)
PY = ESD(2) + XSI(I,J) * ESD(4)
TUTHD(I,J) = X11I(I,J)*PX + X12I(I,J)*PY - Y1I(I,J)
TUPHD(I,J) = X12I(I,J)*PX + X22I(I,J)*PY - Y2I(I,J)
XJ2D(I,J) = THPH(I,J)*TUTHD(I,J) + PHTH(I,J)*TUPHD(I,J)
IF (DABS(XJ2D(I,J)) - PRS) 72,72,73
72 G(I,J) = 0.0
GO TO 75
73 IF (XJ2D(I,J)) 72,72,74
744 IF (XJ2(I,J)*DT+XJ2(I,J)-XJM(I,J)) 72,74,74
74 G(I,J) = GSS(I,J)
75 CKD = DABS(G(I,J) - GS(I,J))
CKK = DABS(G(I,J))
CWK(I) = DMAX1(CWK(I),CKK)
CK(I) = DMAX1(CK(I),CKD)
GS(I,J) = G(I,J)
76 CONTINUE
DIF = DMAX1(CK(I),DIF)
DED = DMAX1(CWK(I),DED)
77 CONTINUE
IF (DIF) 81,81,777
777 IF (DIF/DED - 0.001) 81,81,78
78 ITER = ITER + 1
IF (ITER - 20) 25,25,79
79 WRITE (6,80)
80 FORMAT (1X,18HITERATIONS DIVERGE)
GO TO 500
81 IF(KIP) 1081,1081,1102
1102 IF(NT-NBIFUR) 1081,1081,1100
1100 NCOUNT=NII-NINC
7192 NCOUNT=NCOUNT+NINC
IF(NCOUNT-NIF)1787,1787,1081
1787 SNM=NCOUNT
DO 1101 I=1,N1
AKB(I)=AKB(I,1,I)
AKC(I)=AKB(I,2,I)
110. CONTINUE
CALL SLOP (AKB,DEL,N,AKBP)
CALL SLOP (AKC,DEL,N,AKCP)
DO 7175 I=1,N1
IF(I-N1) 1788,1789,1789
1789 DO 1790 I1 = 1,8

```

```

DO 1791 I2 = 1,8
YMK$ (I1, I2) = 0.0
1791 CONTINUE
1790 CONTINUE
GO TO 7194
1788 AMS(1,6) = AII(3,1,I)
AMS(1,7) = AII(3,3,I)
AMS(3,1) = -PH(I)*XLB
AMS(3,6) = AII(1,1,I)
AMS(3,7) = AII(1,3,I)
AMS(4,3) = -SNN*CS(I)
AMS(4,4) = CT(I)
AMS(5,1) = XNTHP(I)+PH(I)*(XNTH(I)+PST)+XNTH(I)*CT(I)
AMS(5,5) = -PH(I)-CT(I)
AMS(5,6) = 1.0+PHP(I)+PH(I)*PH(I)+AII(3,1,I)*XNTH(I)
AMS(5,7) = AII(3,3,I)*XNTH(I)
AMS(6,1) = XNTH(I)+PST
AMS(6,6) = PH(I)-CT(I)
AMS(7,7) = -CT(I)
AMS(7,8) = SNN*CS(I)
AMS(8,8) = -2.0*CT(I)
DO 1505 III=1,5
DO 1503 JJJ=1,5
DMS(III, JJJ)=0.0
1503 CONTINUE
1505 CONTINUE
DMS(1,1) = -1.0+ PHP(I)+2.0*PH(I)*CT(I) +(AKBI(2,1,I)-XLA*AKBI(1,1,I)
1) *(XNPH(I)+PST)*2.0
DMS(1,2) = 2.0*(XLB* AKBI(2,2,I)-AKBI(1,2,I) -(AKBI(2,1,I)-
1 AKBI(1,1,I)*XLA))
DMS(1,3) = -2.0*SNN*CS(I)*(AKBI(2,1,I)-(AKBI(1,1,I)+AII(1,2,I))*XLA
1+AII(3,2,I))
DMS(1,4) = -2.0*SNN*CS(I)*(AKBI(2,2,I)-XLA*AKBI(1,2,I)+AII(3,4,I)-
1 AII(1,4,I)*XLA)
DMS(1,5) = 2.0*((CT(I)+PH(I))*AKBI(2,1,I)-AKBP(I)*XLA+
1(AKBI(1,1,I)*XLA-AKBI(2,1,I))*(-PH(I)+2.0*CT(I))-AKBI(1,1,I)*CT(I)
2 *XLA)
DMS(2,1) = 1.0
DMS(3,3) = AII(2,2,I)
DMS(3,4) = AII(2,4,I)
DMS(4,1) = SNN*CS(I)
DMS(4,3) = AII(4,2,I)
DMS(4,4) = AII(4,4,I)
DMS(5,1) = CT(I)+PH(I)
DMS(5,5) = 2.0*(AKBI(2,1,I)-AKBI(1,1,I)*XLA)
BMS(1,3) = AII(3,2,I)
BMS(1,4) = AII(3,4,I)
BMS(3,3) = AII(1,2,I)
BMS(3,4) = AII(1,4,I)
BMS(4,1) = -XLB*PH(I)
BMS(4,5) = 2.0*AKBI(1,1,I)
BMS(5,1) = -SNN*XNPH(I)*CS(I)
BMS(5,2) = SNN*CS(I)
BMS(5,3) = 1.0+PH(I)*CT(I)+XNTH(I)*AII(3,2,I)
BMS(5,4) = AII(3,4,I)*XNTH(I)
BMS(6,3) = CT(I)
BMS(6,5) = BMS(5,2)
BMS(7,4) = BMS(6,3)
BMS(8,4) = -BMS(5,2)
EMS(1,1) = SNN*CS(I)*(2.0*CT(I)-3.0*PH(I))
EMS(1,2) = SNN*CS(I)*(2.0*CT(I)*CT(I)-1.0)*XLA
EMS(1,3) = -2.0*SNN*CS(I)*CT(I)*XLA
EMS(1,6) = 2.0*SNN*CS(I)*(AII(1,1,I)*XLA-AII(3,1,I))
EMS(1,7) = 2.0*SNN*CS(I)*(AII(1,3,I)*XLA-AII(3,3,I))
EMS(1,8) = 2.0*(AKCP(I)-(AKBI(2,2,I)-AKBI(1,2,I)*XLA)*CT(I)*2.0
1 +(CT(I)+PH(I))*AKBI(2,2,I)-CT(I)*AKBI(1,2,I)*XLA)
EMS(2,2) = SNN*CS(I)*XLA
EMS(3,3) = -CT(I)
EMS(3,4) = SNN*CS(I)
EMS(3,6) = AII(2,1,I)
EMS(3,7) = AII(2,3,I)
EMS(4,1) = -CT(I)
EMS(4,6) = AII(4,1,I)
EMS(4,7) = AII(4,3,I)
EMS(5,1) = -2.0*SNN*CS(I)
EMS(5,2) = -SNN*CS(I)*CT(I)*XLA
EMS(5,3) = -EMS(5,1)*XLA
EMS(5,4) = EMS(4,1)*XLA

```

```

EMS(5,8) = 2.0*(AKBI(2,2,1)-AKBI(1,2,1)*XLA)
CALL DMINV(DMS,5,DET,LAS,MAS)
CALL DMPRD(DMS,EMS,DES,5,5,8)
CALL DMPRD(BMS,DES,BDES,8,5,8)
DO 7177 IJ1 = 1,8
DO 7176 IJ2 = 1,8
YMK5(IJ1,IJ2) = AMS(IJ1,IJ2)-BDES(IJ1,IJ2)
7176 CONTINUE
7177 CONTINUE
7194 DO 7172 IJ1 = 1,8
DO 7171 IJ2 = 1,8
DELYS = DELZ*YMK5(IJ1,IJ2)
VMS(IJ1,IJ2) = UNNM(IJ1,IJ2) - DELYS
WMS(IJ1,IJ2,1) = UNNM(IJ1,IJ2) + DELYS
7171 CONTINUE
7172 CONTINUE
CALL DMINV(VMS,8,DET,LCS,MCS)
DO 7174 IJ1 = 1,8
DO 7173 IJ2 = 1,8
VMMS(IJ1,IJ2,1) = VMS(IJ1,IJ2)
7173 CONTINUE
7174 CONTINUE
7175 CONTINUE
DO 7180 I = 1,N
IA = I+1
DO 9177 IJ1 = 1,8
DO 9176 IJ2 = 1,8
ALPIS(IJ1,IJ2) = ALPIS(IJ1,IJ2,I)
WMS(IJ1,IJ2) = WMS(IJ1,IJ2,1)
VMS(IJ1,IJ2) = VMMS(IJ1,IJ2,IA)
9176 CONTINUE
9177 CONTINUE
CALL DMPRD(VMS,WMS,VMS,8,8,8)
CALL DMPRD(VMS,ALPS,ANES,8,8,8)
DO 7179 IJ1 = 1,8
DO 7178 IJ2 = 1,8
ALPIS(IJ1,IJ2,IA) = ANES(IJ1,IJ2)
7178 CONTINUE
7179 CONTINUE
7180 CONTINUE
GAMS(1,1) = ALPIS(1,6,N1)+ALPIS(1,1,N1)*A11+ALPIS(1,2,N1)*A31+
1 ALPIS(1,3,N1)*A21+ALPIS(1,4,N1)*A41
GAMS(1,2) = ALPIS(1,5,N1)+ALPIS(1,1,N1)*A12+ALPIS(1,2,N1)*A32+
1 ALPIS(1,3,N1)*A22+ALPIS(1,4,N1)*A42
GAMS(1,3) = ALPIS(1,7,N1)+ALPIS(1,1,N1)*A13+ALPIS(1,2,N1)*A33+
1 ALPIS(1,3,N1)*A23+ALPIS(1,4,N1)*A43
GAMS(1,4) = ALPIS(1,8,N1)+ALPIS(1,1,N1)*A14+ALPIS(1,2,N1)*A34+
1 ALPIS(1,3,N1)*A24+ALPIS(1,4,N1)*A44
GAMS(2,1) = ALPIS(2,6,N1)+ALPIS(2,1,N1)*A11+ALPIS(2,2,N1)*A31+
1 ALPIS(2,3,N1)*A21+ALPIS(2,4,N1)*A41
GAMS(2,2) = ALPIS(2,5,N1)+ALPIS(2,1,N1)*A12+ALPIS(2,2,N1)*A32+
1 ALPIS(2,3,N1)*A22+ALPIS(2,4,N1)*A42
GAMS(2,3) = ALPIS(2,7,N1)+ALPIS(2,1,N1)*A13+ALPIS(2,2,N1)*A33+
1 ALPIS(2,3,N1)*A23+ALPIS(2,4,N1)*A43
GAMS(2,4) = ALPIS(2,8,N1)+ALPIS(2,1,N1)*A14+ALPIS(2,2,N1)*A34+
1 ALPIS(2,3,N1)*A24+ALPIS(2,4,N1)*A44
GAMS(3,1) = ALPIS(3,6,N1)+ALPIS(3,1,N1)*A11+ALPIS(3,2,N1)*A31+
1 ALPIS(3,3,N1)*A21+ALPIS(3,4,N1)*A41
GAMS(3,2) = ALPIS(3,5,N1)+ALPIS(3,1,N1)*A12+ALPIS(3,2,N1)*A32+
1 ALPIS(3,3,N1)*A22+ALPIS(3,4,N1)*A42
GAMS(3,3) = ALPIS(3,7,N1)+ALPIS(3,1,N1)*A13+ALPIS(3,2,N1)*A33+
1 ALPIS(3,3,N1)*A23+ALPIS(3,4,N1)*A43
GAMS(3,4) = ALPIS(3,8,N1)+ALPIS(3,1,N1)*A14+ALPIS(3,2,N1)*A34+
1 ALPIS(3,3,N1)*A24+ALPIS(3,4,N1)*A44
GAMS(4,1) = ALPIS(4,6,N1)+ALPIS(4,1,N1)*A11+ALPIS(4,2,N1)*A31+
1 ALPIS(4,3,N1)*A21+ALPIS(4,4,N1)*A41
GAMS(4,2) = ALPIS(4,5,N1)+ALPIS(4,1,N1)*A12+ALPIS(4,2,N1)*A32+
1 ALPIS(4,3,N1)*A22+ALPIS(4,4,N1)*A42
GAMS(4,3) = ALPIS(4,7,N1)+ALPIS(4,1,N1)*A13+ALPIS(4,2,N1)*A33+
1 ALPIS(4,3,N1)*A23+ALPIS(4,4,N1)*A43
GAMS(4,4) = ALPIS(4,8,N1)+ALPIS(4,1,N1)*A14+ALPIS(4,2,N1)*A34+
1 ALPIS(4,3,N1)*A24+ALPIS(4,4,N1)*A44
C THE MATRIX GAMS IS MULTIPLIED BY 10**-10
7183 DO 7746 I1=1,4
DO 7747 I2=1,4
GAMS(I1,I2) = GAMS(I1,I2)*0.000000001
7747 CONTINUE
7746 CONTINUE

```

```

C  CALCULATION OF THE DETERMINATE OF GAMS, DENOTED BY DET1
CALL DMINV(GAMS,4,DET1,MGAS1,MGAS2)
WRITE(6,7195) NCOUNT,DET1,PST
7195 FORMAT(' NCOUNT=',I3,'      DET1 =',E13.5,'      PST =',E15.7)
GO TO 7192
1081 DO 83 I = 1,M1
      U(I) = U(I) + UMD(2,I)*DT
      W(I) = W(I) + UMD(3,I)*DT
      PH(I) = PH(I) + UMD(1,I)*DT
      XNTH(I) = XNTH(I) + UMD(4,I)*DT
      XNPH(I) = XNPH(I) + VDI(1,I)*DT
      Q(I) = Q(I) + UMD(5,I)*DT
      XMTH(I) = XMTH(I) + UMD(6,I)*DT
      XMPH(I) = XMPH(I) + VDI(2,I)*DT
      DO 82 J = 1,M1
        TUTH(I,J) = TUTH(I,J) + TUTHD(I,J)*DT
        TUPH(I,J) = TUPH(I,J) + TUPHD(I,J)*DT
82 CONTINUE
83 CONTINUE
C  CALCULATION OF AVERAGE RADIAL DEFORMATION, WAVE
CALL INT(W,DEL,N,WINT)
WAVE = WINT/TAX
GO TO 403
500 STOP
END
/*
//GO.SYSIN DD *

```

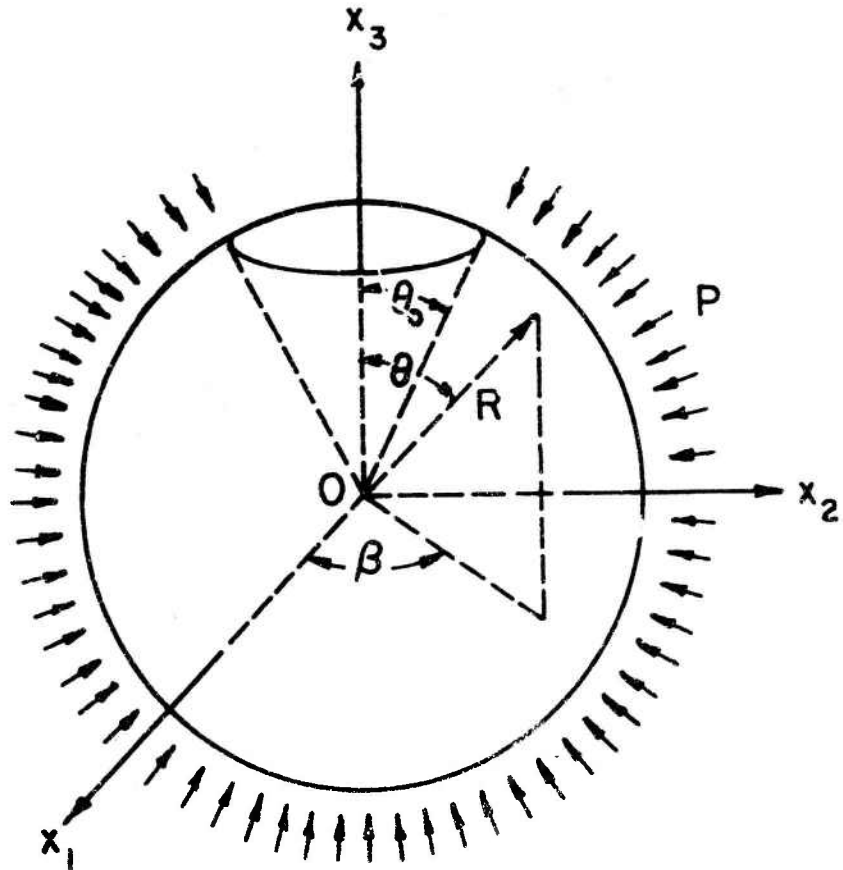


Fig. 1 The geometry of the shell.

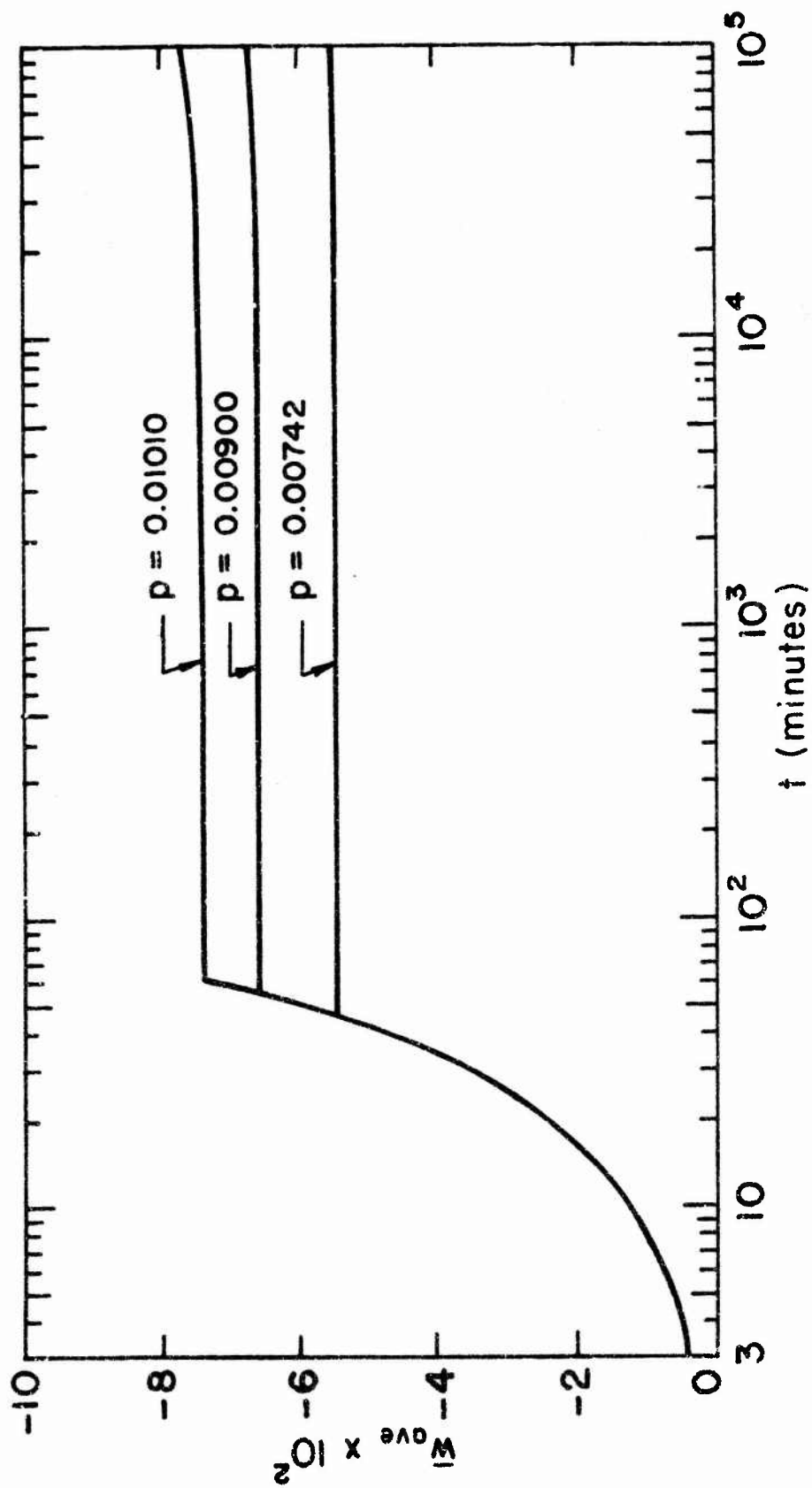


Fig. 2. \bar{w}_{ave} vs. t curves.

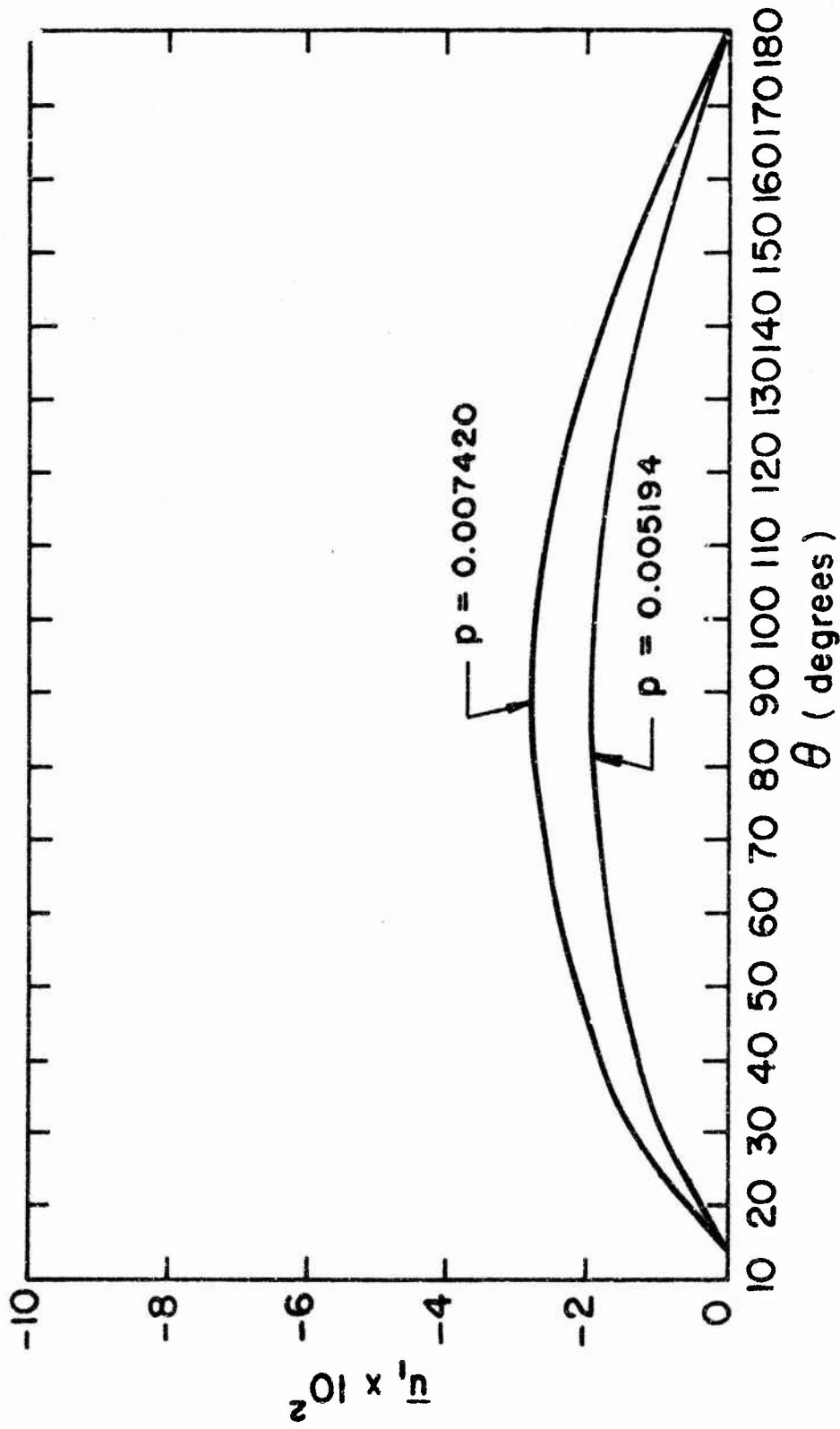


Fig. 3. \bar{u}_1 vs. θ for $p = 0.005194$ and 0.007420 .

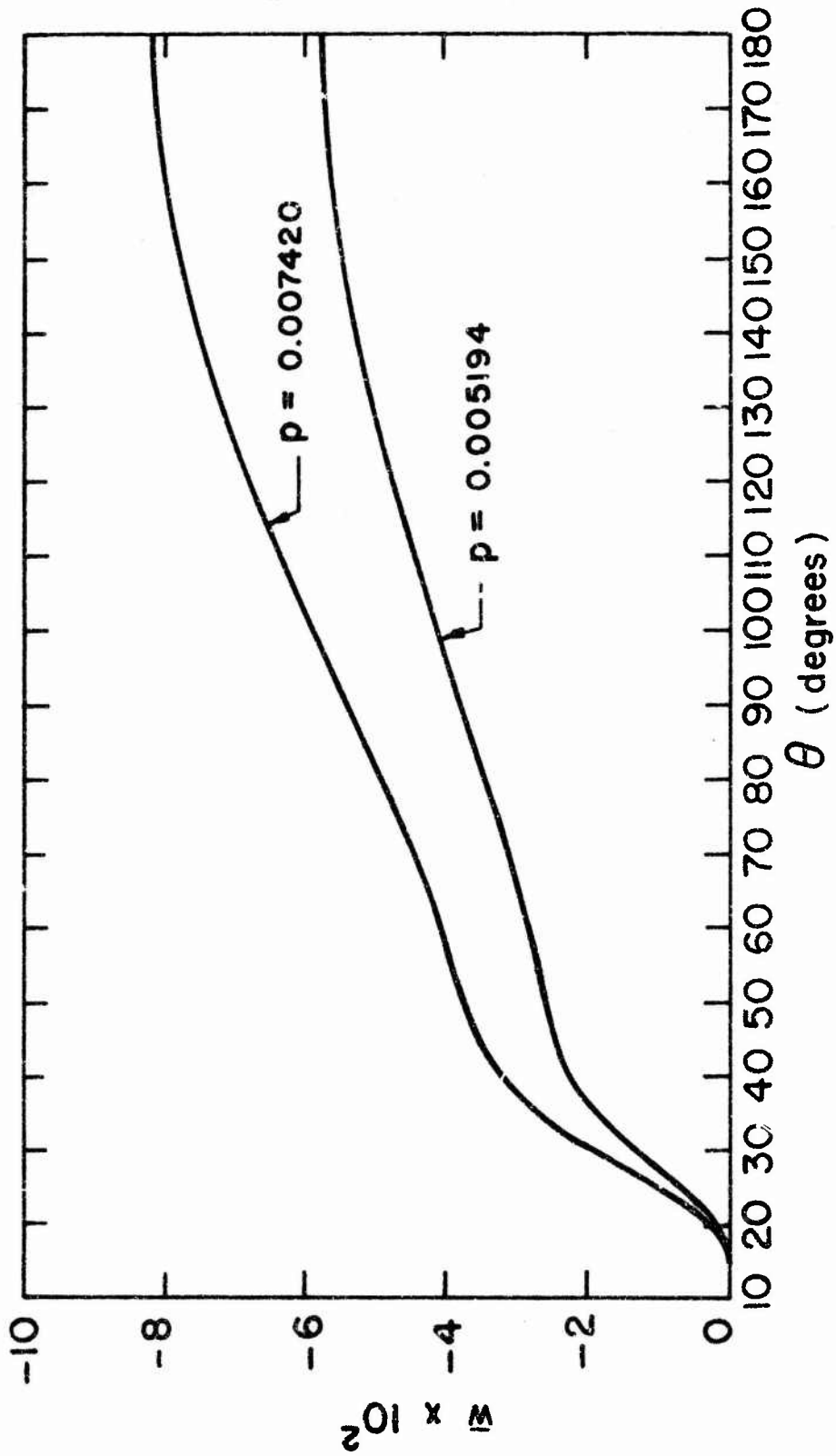


Fig. 4. \bar{w} vs. θ curves for $p = 0.005194$ and 0.007420 .

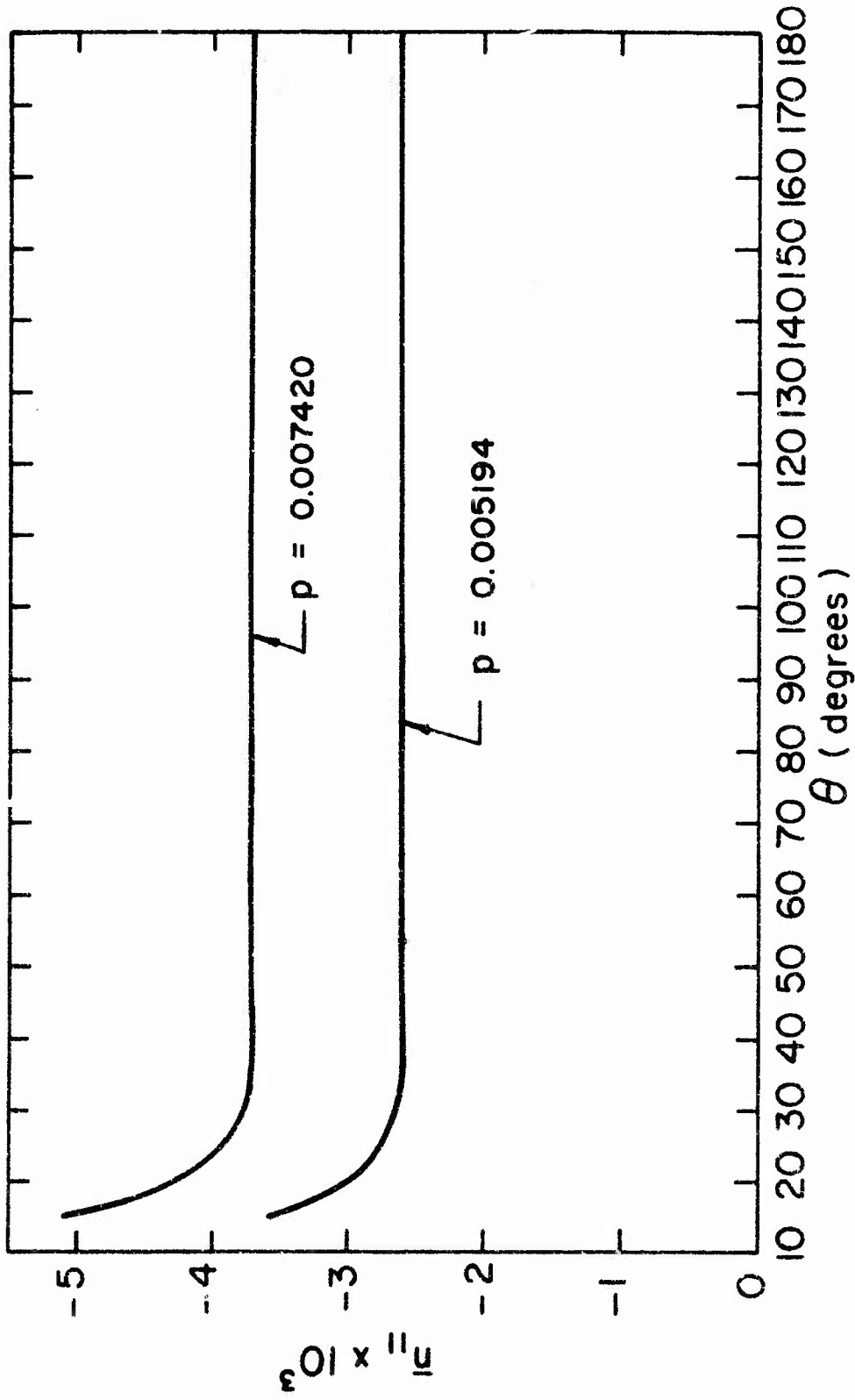


Fig. 5. \bar{n}_{11} vs. θ curves for $p = 0.005194$ and 0.007420 .

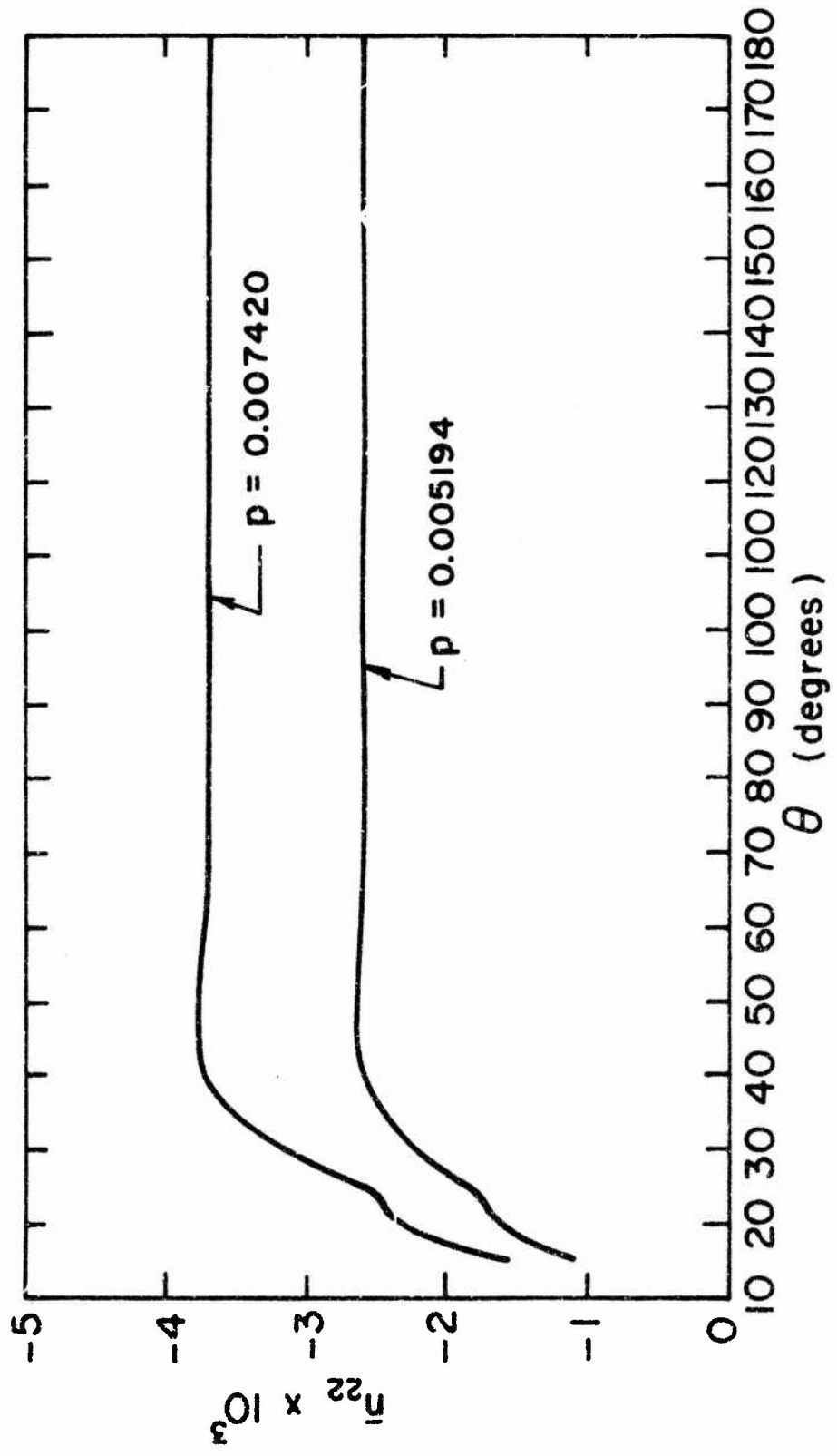


Fig. 6. \bar{n}_{22} vs. θ curves for $p = 0.005194$ and 0.007420 .

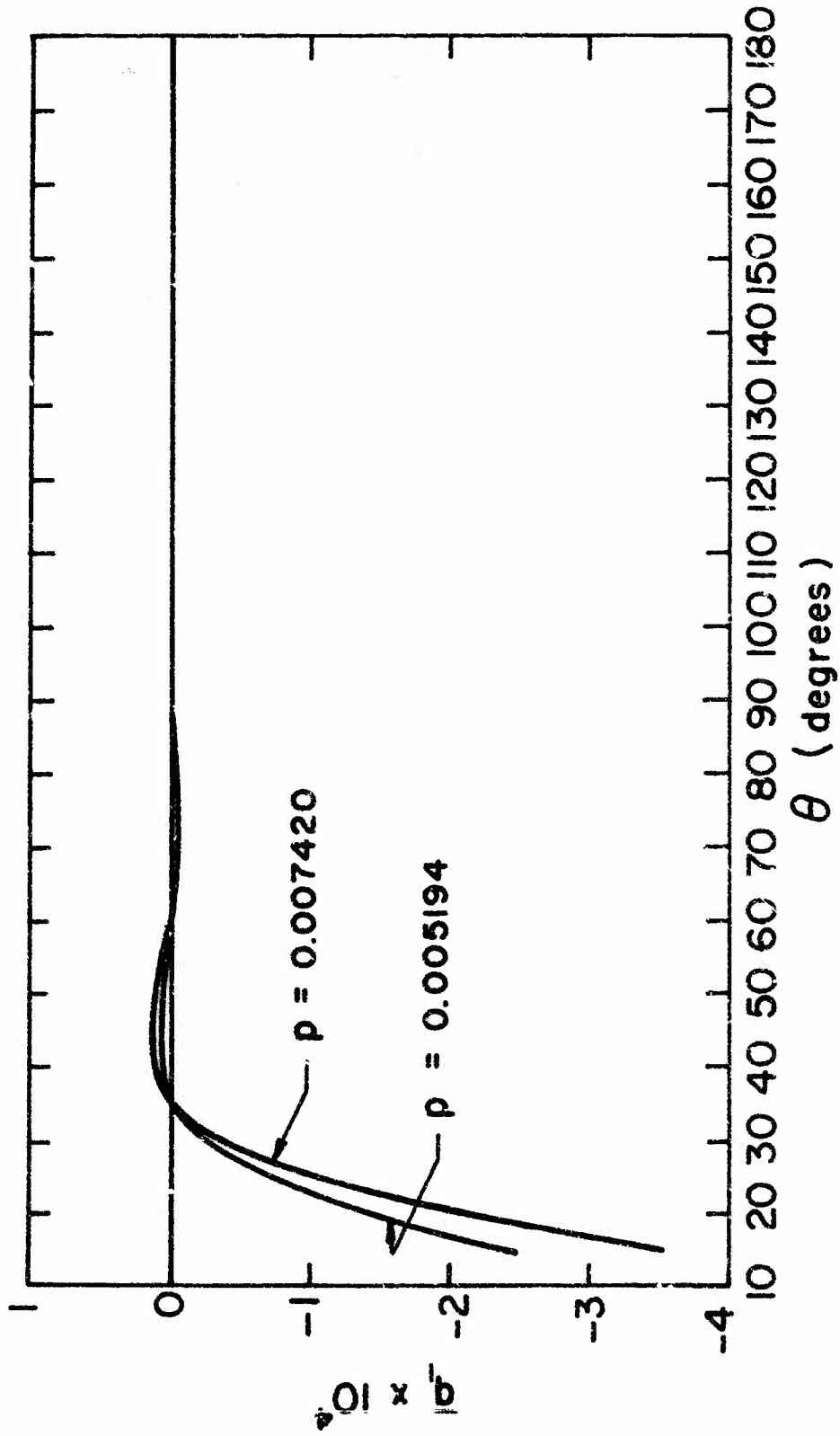


Fig. 7. q_1 vs. θ curves for $p = 0.005194$ and 0.007420 .

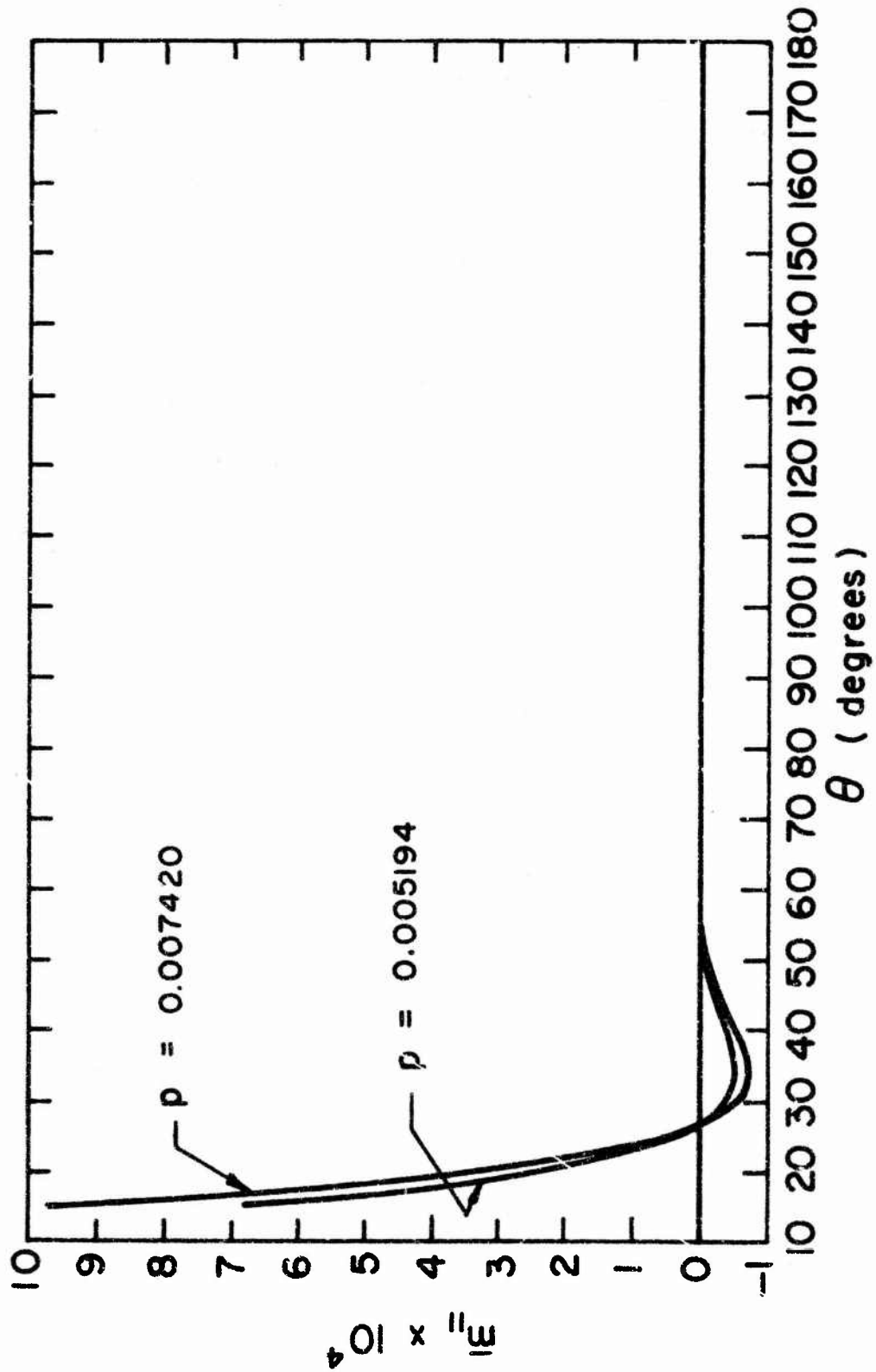


Fig. 8. \bar{m}_{11} vs. θ curves for $p = 0.005194$ and $p = 0.007420$.

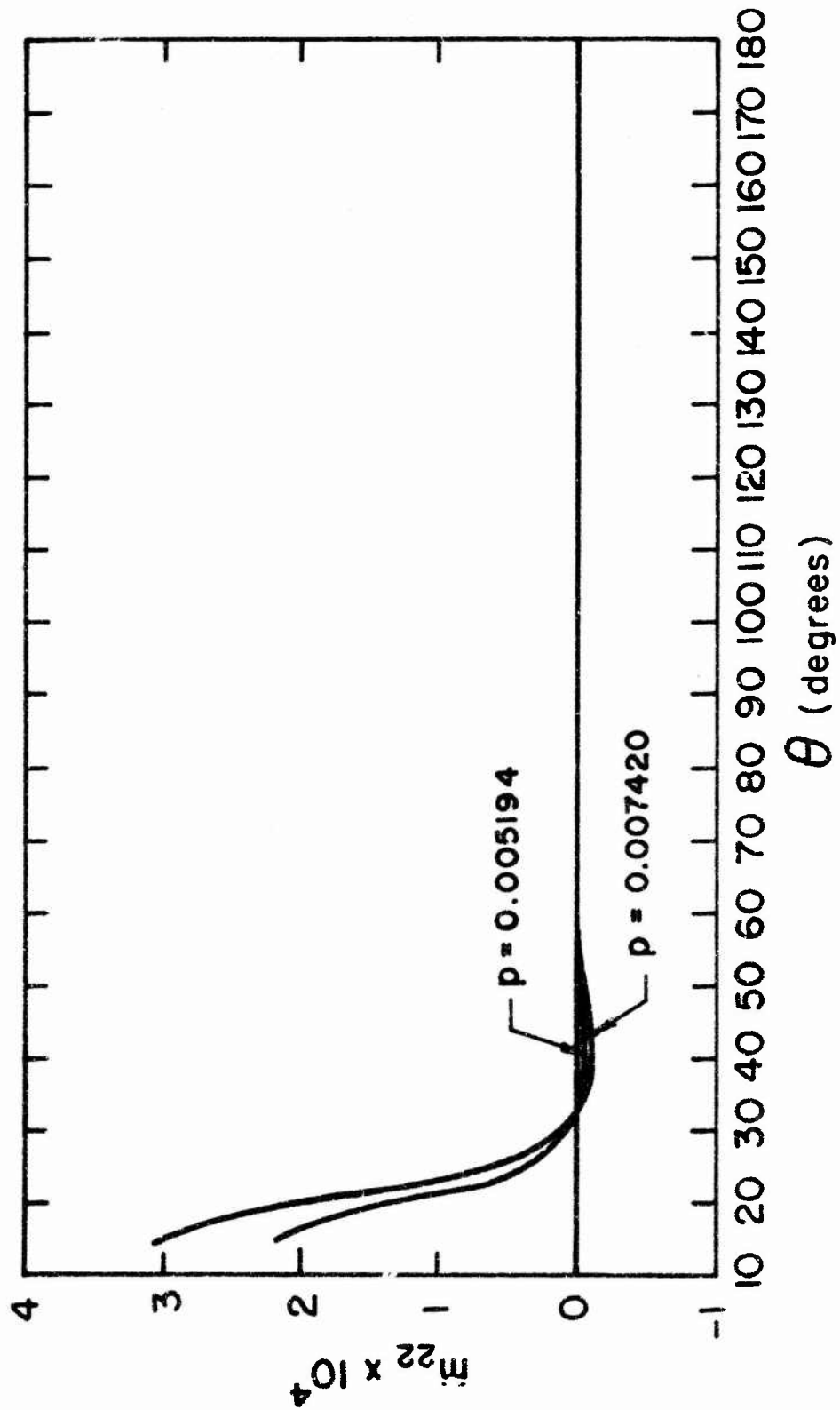


Fig. 9. \bar{m}_{22} vs. θ curves for $p = 0.005194$ and 0.007420 .

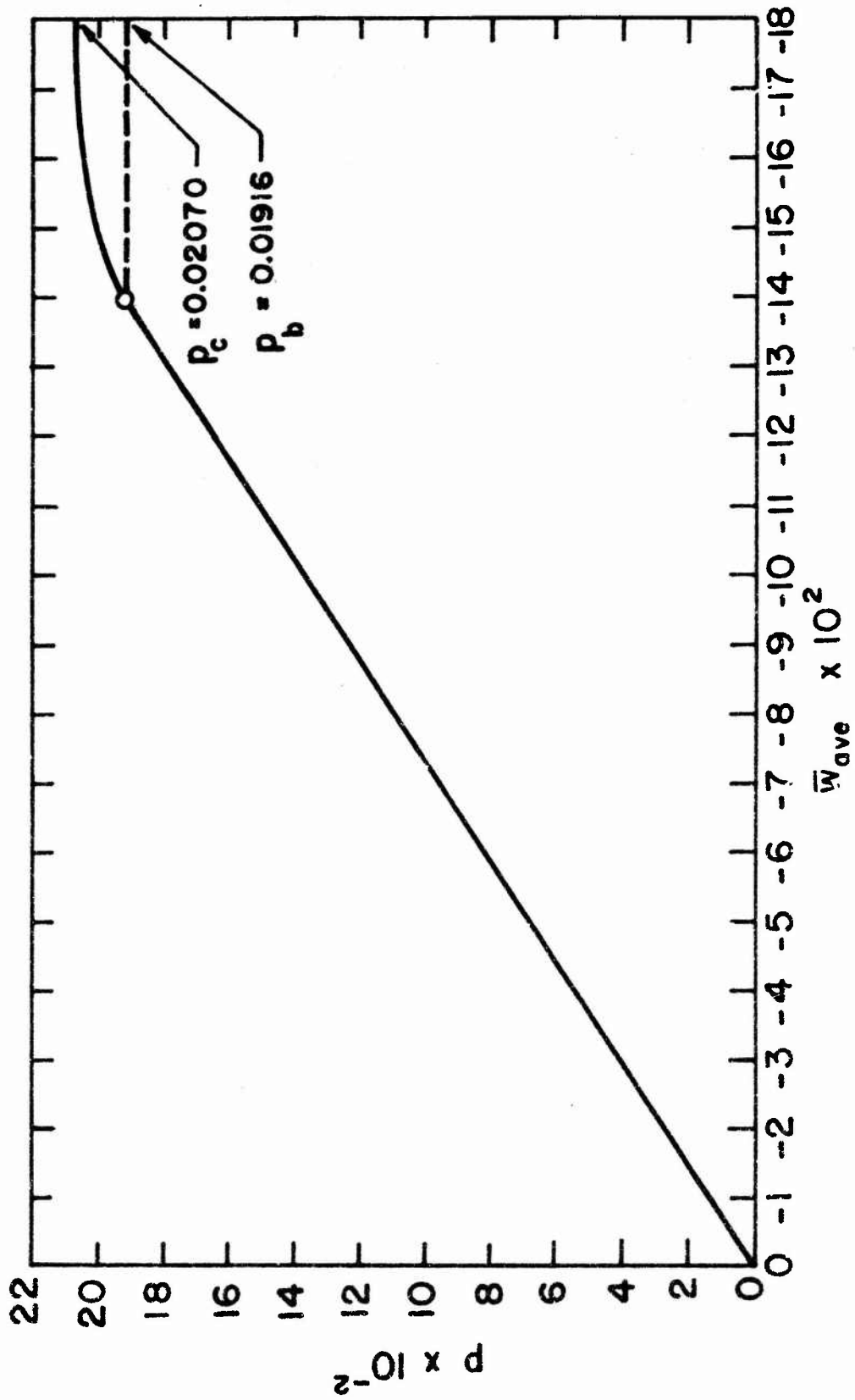


Fig. 10. p vs. \bar{W}_{ave} curve.